Reviewed Preprint
v1 • January 12, 2026
Not revised

Reviewed Preprint
v2 • July 17, 2026
Revised by authors

Symmetric brain-liver circuits mediate lateralized regulation of hepatic glucose output in mice

Zhonglong Wang[1,2,*], Xiangfei Gong[1,2,*], Li Jiang[1,2,*], Ke Wang[1,2,*], Xinyuan Sun[1,2], Yingxi Li[1,2], Mengtong Ran[1,2], Yanshen Chen[1,2], Hongdong Wang[3], Xuehui Chu[4], Shun Wang[1,2], Junjie Wang[1,2], Xiao Zheng[1,2] ✉, Haiping Hao[1,2] ✉, Hao Xie[1,2] ✉

[1]College of Pharmacy, China Pharmaceutical University, Nanjing, China • [2]State Key Laboratory of Natural Medicines, Institute of innovative Drug Discovery and Development, Jiangsu Provincial Key Laboratory of Targetome and Innovative Drugs, China Pharmaceutical University, Nanjing, China • [3]Department of Endocrinology, Endocrine and Metabolic Disease Medical Center, Nanjing Drum Tower Hospital, Affiliated Hospital of Medical School, Nanjing University, Nanjing, China • [4]Department of Pancreatic and Metabolic Surgery, Nanjing Drum Tower Hospital, Affiliated Hospital of Medical School, Nanjing University, Nanjing, China

✉ **For correspondence:**
xiaozheng@cpu.edu.cn
haipinghao@cpu.edu.cn
haoxie@cpu.edu.cn

* These authors contributed equally

Competing interests: No competing interests declared

Funding: See page 21

Reviewing editor: Christoph Buettner, Rutgers Robert Wood Johnson Medical School, United States

eLife Assessment

This **important** study combines anatomical tracing, tissue clearing, and functional manipulations to demonstrate lateralized brainstem control of hepatic glucose metabolism and identify a site of sympathetic nerve crossover supplying the liver. The evidence supporting the anatomical organization of hepatic sympathetic innervation is **compelling**, and the functional studies provide **solid** support for a role of asymmetric sympathetic outflow in regulating glucose homeostasis. While some uncertainty remains regarding the contribution of sensory innervation and the extent to which these findings generalize beyond mice, the work provides an invaluable advance in understanding neural regulation of liver metabolism.

https://doi.org/10.7554/eLife.109599.2.sa3

Abstract

Neural lateralization is well recognized in the control of contralateral somatic movement, yet its relevance to visceral organ regulation remains poorly understood. This study aimed to determine whether the central nervous system exerts lateralized control over hepatic glucose metabolism and to localize the site of peripheral sympathetic crossover to the liver. Pseudorabies virus (PRV) tracing revealed bilateral projections from the lateral paragigantocellular nucleus (LPGi) with preferential innervation of the contralateral hepatic lobes. Unilateral LPGi activation elevated systemic glucose by enhancing glycogenolysis and gluconeogenesis specifically in contralateral lobes, whereas bilateral activation produced additive effects. Following unilateral hepatic denervation, contralateral LPGi activation induced metabolic compensation in the remaining innervated lobes, characterized by increased norepinephrine release, glucose production, and glycogen depletion. Whole-mount tissue clearing and dual viral tracing localized the sympathetic crossover to the porta hepatis. Developmental analysis showed that lobar-specific innervation along the vasculature emerges by postnatal week 2. These findings demonstrate that the brainstem can exert lobe-specific, lateralized control of hepatic glucose metabolism via bilaterally projecting brain – liver sympathetic pathways. This contralateral regulation arises from a peripheral decussation at the porta hepatis, and the compensatory activation observed after denervation reveals an intrinsic neuroadaptive mechanism that helps safeguard systemic glucose homeostasis.

Highlights

- Brain-liver sympathetic projections exhibit predominant contralateral innervation
- Unilateral LPGi activation drives glucose production in contralateral hepatic lobes
- Unilateral denervation augments contralateral LPGi-mediated metabolic compensation
- Sympathetic crossover to the liver localizes at the porta hepatis

Introduction

Pronounced functional lateralization within the central nervous system (CNS) is a well-documented phenomenon,[1,2] traditionally associated with cognitive and motor processes such as language, voluntary movement, and spatial navigation.[3,4] Emerging evidence indicates that this lateralization extends beyond cortical functions to the autonomic regulation of visceral organs, thereby enhancing the efficiency of physiological responses.[5–7] Such CNS specialization allows for optimized resource allocation and context-dependent prioritization of functional outputs. For instance, paired organs such as kidneys and adrenal glands receive predominantly contralateral neural inputs, enabling coordinated bilateral function.[8,9] Previous studies have shown that the left hemisphere preferentially modulates sympathetic outflow to the right kidney and *vice versa*,[8,10] and that cortical projections to the adrenal medulla are primarily contralateral, with the rostral cingulate motor area as a bilateral exception.[9] However, the influence of neural lateralization on structurally asymmetric visceral organs remains incompletely understood and appears to be organ-specific. The heart, for instance, exhibits distinct lateralized autonomic innervation: left-sided fibers predominantly mediate chronotropic regulation via the sinoatrial node, whereas right-sided fibers exert greater inotropic and dromotropic functions.[6,11] Additionally, cortical neurons regulating gastric sympathetic function are predominantly localized in the right hemisphere, whereas parasympathetic control displays only a modest right-sided predominance.[7,12] These examples underscore the organ-specific nature of lateralized autonomic neural projections.

The liver, as the largest asymmetrical visceral organ, plays a central role in systemic metabolic homeostasis,[13,14] orchestrating physiological processes such as glucose production, lipid metabolism, protein synthesis, and detoxification.[16,17] In mice, hepatic innervation first appears in extrahepatic bile ducts at embryonic day 17.5 and extends into lobes during the early postnatal period,[18] yet the precise pattern of this innervation remains unknown. Previous anatomical and functional studies, including our own, have established that the liver receives dense sympathetic innervation from postganglionic neurons of the celiac-superior mesenteric ganglia (CG-SMG).[19,20,21,22] Within this context, the brainstem lateral paragigantocellular nucleus (LPGi) has been identified as a key node in the regulation of hepatic sympathetic tone and glucose output.[20] However, whether this regulation is lateralized and lobe-specific, and where sympathetic crossover occurs, has not been systematically defined.

To address these gaps, we applied retrograde trans-synaptic tracing with pseudorabies virus (PRV) to delineate LPGi projections to hepatic lobes and assess their lateralization.[21–23] Functional experiments employing chemogenetic and optogenetic activation of LPGi neurons clarified the physiological impact of this neural circuitry on hepatic glucose production (HGP). Additionally, we identified compensatory neural mechanisms that maintain systemic glucose homeostasis following unilateral disruption of the neural circuit regulating hepatic innervation. Whole-mount clearing identified the porta hepatis as the site of sympathetic crossover and revealed developmental axon extension of hepatic fibers along the vasculature. Together, these findings reveal that lateralized neuronal circuits exert lobe-specific control over hepatic glucose output and recruit neuroadaptive responses to preserve metabolic homeostasis following unilateral disruption.

Results

1. Contralateral projections from the LPGi to distinct hepatic lobes

Previous studies of intrahepatic innervation mainly focused on individual lobes, such as the left or right lateral lobes in mice.[14,15] We first asked whether sympathetic innervation is a uniform feature across all lobes. To address this, we examined the intact mouse liver using tissue clearing combined with immunofluorescence staining of tyrosine hydroxylase (TH), the rate-limiting enzyme in catecholamine synthesis. This analysis revealed that, although hepatic lobes differ in volume (Figure 1A), sympathetic fibers consistently branch into all lobes with comparable density (Figure 1A). To further investigate the anatomical basis of central neural regulation of the liver, we performed multi-synaptic retrograde tracing by injecting PRV into individual hepatic lobes, including the left lateral, median, right posterior, right anterior, and caudate lobes (Figures S1A and S1B). Five days post-injection, PRV-labeled neurons were consistently identified in the LPGi of the brainstem (Figure 1B, Figures S1C-S1F). Quantitative analyses revealed a clear contralateral dominance: the injection into left lateral and median lobes yielded approximately twice as many labeled neurons in the right LPGi as in the left, whereas the injection into right posterior, right anterior, and caudate lobes preferentially labeled neurons in the left LPGi (Figure 1C). These findings provide direct anatomical evidence of a symmetric projection pattern in which each LPGi hemisphere preferentially innervates contralateral hepatic lobes (Figure 1D). Based on their robust lateralization, the right anterior and median lobes were selected as representative targets for subsequent analyses.

To validate these projection patterns, we performed dual labeling by co-injecting PRV-CAG-EGFP into the right anterior lobe and PRV-CAG-mRFP into the median lobe. In the left LPGi, 73.7% of PRV-positive neurons expressed EGFP, showing projections to the right anterior lobe, whereas in the right LPGi, 62.5% expressed mRFP, indicating projections to the median lobe (Figures 1E and 1F). A subset of neurons displayed co-labeling, suggesting that although the predominant projection pattern is contralateral, a population of LPGi neurons innervates both lobes bilaterally. These findings establish a contralaterally biased projection pattern from each LPGi to distinct hepatic lobes, providing the anatomical foundation for lateralized brain-liver circuits that regulate hepatic glucose metabolism.

Because PRV tracing cannot distinguish sympathetic efferent from vagal sensory pathways, we next sought to determine the circuit identity of liver-projecting LPGi neurons. Unlike the NTS, a well-established hepatic sensory center served here as a positive control,[24] the LPGi contained few CGRP-positive cell bodies (Figure S1G). Moreover, co-injection of hSyn-cre and DIO-Axon-EGFP into the LPGi did not yield Axon-EGFP-positive signals in either the dorsal root ganglia (DRG) or nodose ganglia (NG) (Figures S1H-S1J). Together, these findings indicate that the LPGi specifically regulates sympathetic, rather than vagal sensory, inputs to the liver.

2. Differential HGP by LPGi lateralization

To assess the functional implications of this anatomical laterality, we examined whether activation of the LPGi in each hemisphere modulates HGP in a lobe-specific manner. Prior single-nucleus RNA sequencing and immunofluorescence analyses demonstrated that liver-projecting LPGi neurons are predominantly GABAergic,[45] we selectively activated these neurons unilaterally or bilaterally using chemogenetics (Figure 2A, Figure S2A). LPGi activation significantly increased blood glucose, with area under the curve (AUC) increases by 27%, 34%, and 52% following left-, right-, and bilateral stimulation, respectively (Figure 2A). Moreover, right-sided activation induced greater hyperglycemia than left-sided stimulation, possibly reflecting differences in the metabolic capacity or volume of the contralateral hepatic lobes (Figure 1A).

At the molecular level, one hour following stimulation, phosphorylation of glycogen phosphorylase (pPYGL) and glycogen synthase (pGS) increased in contralateral lobes, as assessed by immunofluorescence and western blot. Left LPGi activation preferentially enhanced pPYGL and pGS levels in the right anterior lobe compared with right-sided activation, whereas right LPGi

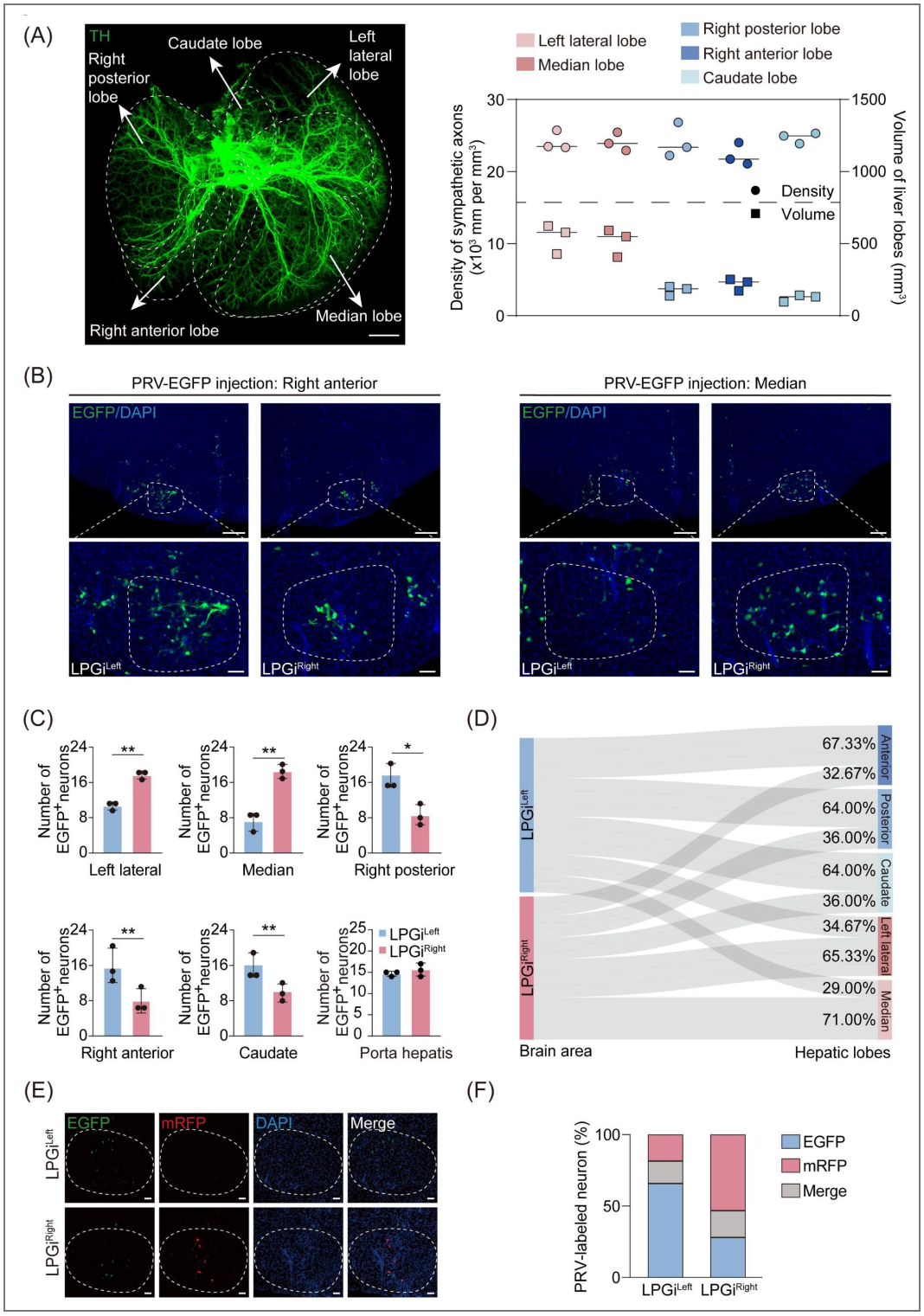

Figure 1. The brain contralaterally projects to the liver.

(A) Representative 3D images of TH-immunostained mouse liver (left), with quantification of sympathetic axon density and lobe volume (right). Scale bar, 3,000 μm. (B) Representative immunofluorescence images of PRV-labeled neurons (EGFP) in the left and right LPGi following PRV injections into the right anterior (left) and median (right) lobes. Scale bars, 200μm (top) and 100 μm (bottom). (B) Quantification of PRV-labeled neurons in left and right LPGi across different hepatic lobes: left lateral, median, right posterior, right anterior, caudate, and porta hepatis (n = 3). (D) Sankey diagram showing projection patterns from left and right LPGi to individual hepatic lobes. (E and F) Representative slices of $EGFP^+$ and $mRFP^+$ neurons in left (top) and right (bottom) LPGi following PRV-EGFP (right anterior lobe) and PRV-mRFP (median lobe) injections. Proportions of $EGFP^+$, $mRFP^+$, and co-labeled neurons in left and right LPG (F, n = 3). Scale bars, 100 μm. Data are expressed as means ± SEM, with individual values shown for all experiments. * $p < 0.05$, ** $p < 0.01$. Unpaired Student's t-test for (C).

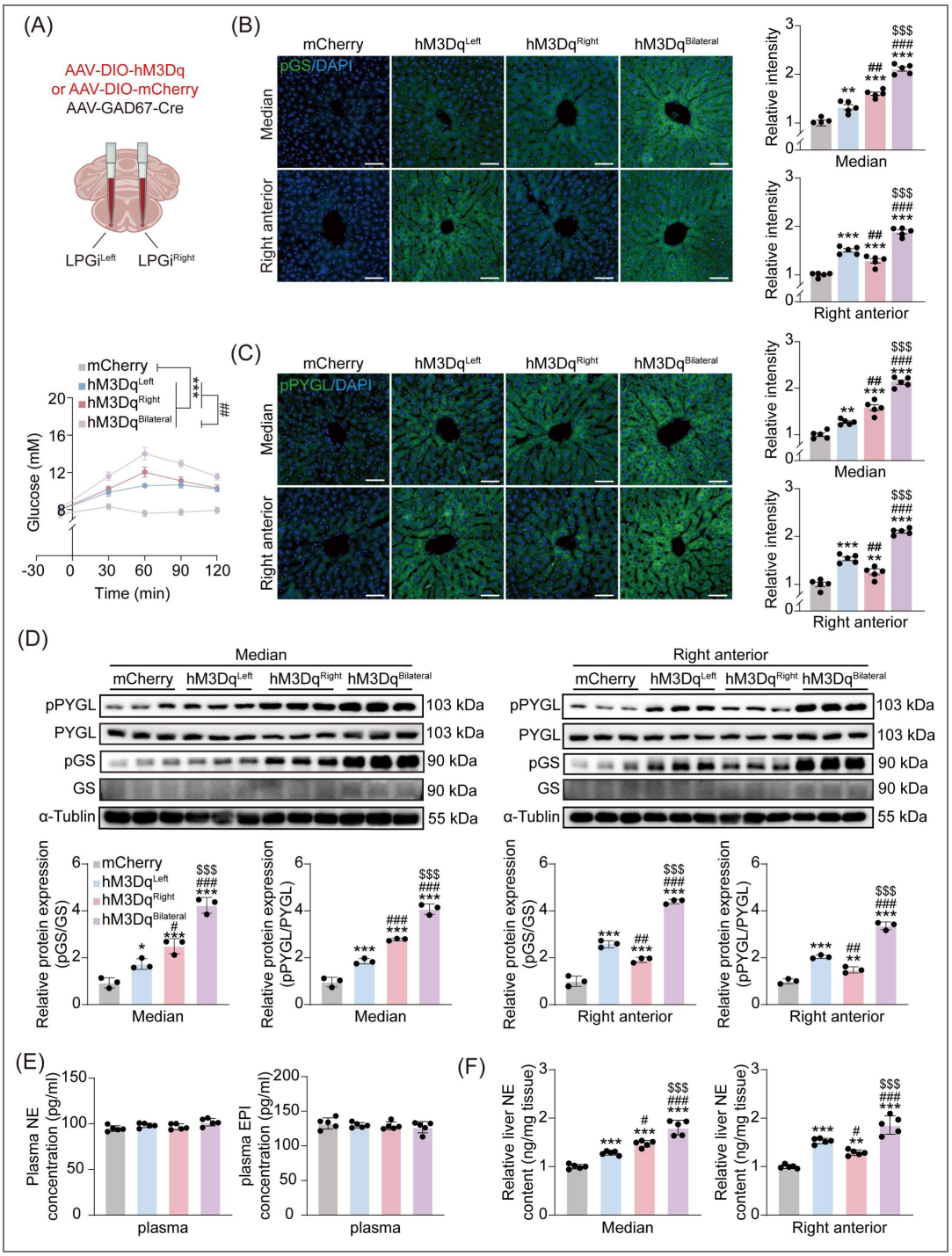

Figure 2. LPGi stimulation raises blood glucose by driving contralateral, lobe-specific hepatic glycogenolysis.

(A) Scheme for injecting AAV-DIO-hM3Dq or AAV-DIO-mCherry (top). Blood glucose levels following chemogenetic activation of the left, right, or bilateral LPGi, measured at −10, 30, 60, 90, and 120 min (bottom, *n* = 6). (B and C) Representative immunofluorescence images of pGS (B) and pPYGL (C) expression in the median (top) and right anterior (bottom) lobes after 1 h chemogenetic activation of left, right, or bilateral LPGi, with quantification of relative fluorescence intensity (*n* = 4-5). Scale bars, 100 μm. (D) Western blot analysis of pPYGL, PYGL, pGS, and GS in median (left) and right anterior (right) lobes after 1 h activation, with densitometric quantification (bottom, *n* = 3). (E) Plasma concentrations of norepinephrine (NE) (left, *n* = 5) and epinephrine (EPI) (right, *n* = 5) following 1 h activation. (F) NE contents in median (left, *n* = 5) and right anterior (right, *n* = 5) lobes after 1 h activation. Data are expressed as means ± SEM, with individual values shown for all experiments. * $p < 0.05$, ** $p < 0.01$, *** $p < 0.001$; # $p < 0.05$, ## $p < 0.01$, ### $p < 0.001$; $$$ $p < 0.001$. One-way ANOVA with the Tukey test for (A-F).

activation exerted a greater effect in the median lobe relative to left-sided stimulation (Figures 2B-2D). Bilateral stimulation further amplified pPYGL and pGS expression in both lobes compared with unilateral activation. PAS staining confirmed glycogen depletion in metabolically engaged contralateral lobes (Figure S2B). In terms of gluconeogenesis, enzymatic activity assays revealed increased phosphoenolpyruvate carboxykinase (PEPCK) and glucose-6-phosphatase (G6PC) activity in hepatic lobes undergoing enhanced glycogenolysis, despite unchanged protein levels within the one-hour window (Figures S2C-S2F).

To exclude contributions from systemic endocrine responses, particularly those mediated by the hypothalamic-pituitary-adrenal (HPA) axis, we measured plasma NE, EPI, insulin, and glucagon 1 hour after LPGi activation. None of these hormones was significantly altered by either unilateral or bilateral stimulation (Figure 2E and Figure S2G). In contrast, intrahepatic NE content rose specifically in contralateral lobes: by 1.49-fold in the right anterior lobe after left LPGi activation, 1.53-fold in the median lobe after right LPGi activation, and over 1.85-fold in both lobes after bilateral activation (Figure 2F). These findings support a mechanism in which lobe-specific sympathetic activation drives hepatic glucose output in a lateralized manner, independent of systemic hormonal changes.

To achieve higher temporal precision, we applied optogenetics by delivering AAV9-GAD67-Cre with AAV9-DIO-ChR2-mCherry viruses to the LPGi (Figure S3A, Figure S4A). Compared with chemogenetics, optogenetic activation elicited greater hyperglycemia, with AUC rising by 32%, 42%, and 62% for left-, right-, and bilateral stimulation, respectively (Figure S3A). Molecular and histological analyses paralleled those from chemogenetics, including contralateral and additive effects on pPYGL and pGS (Figures S3B-S3D), glycogen depletion (Figure S4B), elevated intrahepatic NE content (Figure S3F), and enhanced PEPCK and G6PC activity (Figures S4C-S4F), without changes in plasma catecholamines (Figure S3E). Taken together, these findings demonstrate that each LPGi hemisphere preferentially drives glucose production in contralateral hepatic lobes, primarily through localized sympathetic activation and glycogenolysis in contralateral hepatic regions.

3. Compensatory neural responses following unilateral hepatic denervation

While compensatory adaptations following unilateral damage are well described in symmetrical organs, it remains unclear whether similar mechanisms operate in asymmetrical organs such as the liver.[26–28] To test this, we chemically denervated the right- or left-sided lobes using 6-OHDA. Despite the absence of directly sympathetic input to denervated lobes, systemic blood glucose levels were unchanged compared with controls (Figures 3A-3C, Figure S5A), indicating functional compensation through the remaining intact liver. Further analyses revealed increased expression of pPYGL and pGS, as well as elevated intrahepatic NE levels and glycogen depletion in non-denervated hepatic lobes (Figures 3D-3H, Figures S5B-S5E).

To elucidate the underlying mechanism, we quantified c-FOS expression in the LPGi following unilateral hepatic denervation. Right-sided lobes denervation increased c-FOS in the left LPGi, and *vice versa* (Figure 3I), suggesting that contralateral LPGi upregulates its sympathetic output to intact ipsilateral hepatic lobes, thereby compensating for the loss of innervation in denervated lobes. Together, these findings identify a neuroadaptive mechanism in which the ipsilateral LPGi augments sympathetic output to intact hepatic lobes, thereby maintaining systemic glucose homeostasis despite partial intrahepatic neural disruption.

4. Peripheral decussation of sympathetic hepatic control at the porta hepatis

Contralateral neural circuitry typically arises from central decussations, such as corticospinal tracts that cross at the pyramids for limb motor control,[29,30] and visual pathways that decussate at the optic chiasm for hemispheric processing of visual fields.[31] Whether the brain's contralateral regulation of the liver occurs centrally or peripherally, however, has remained

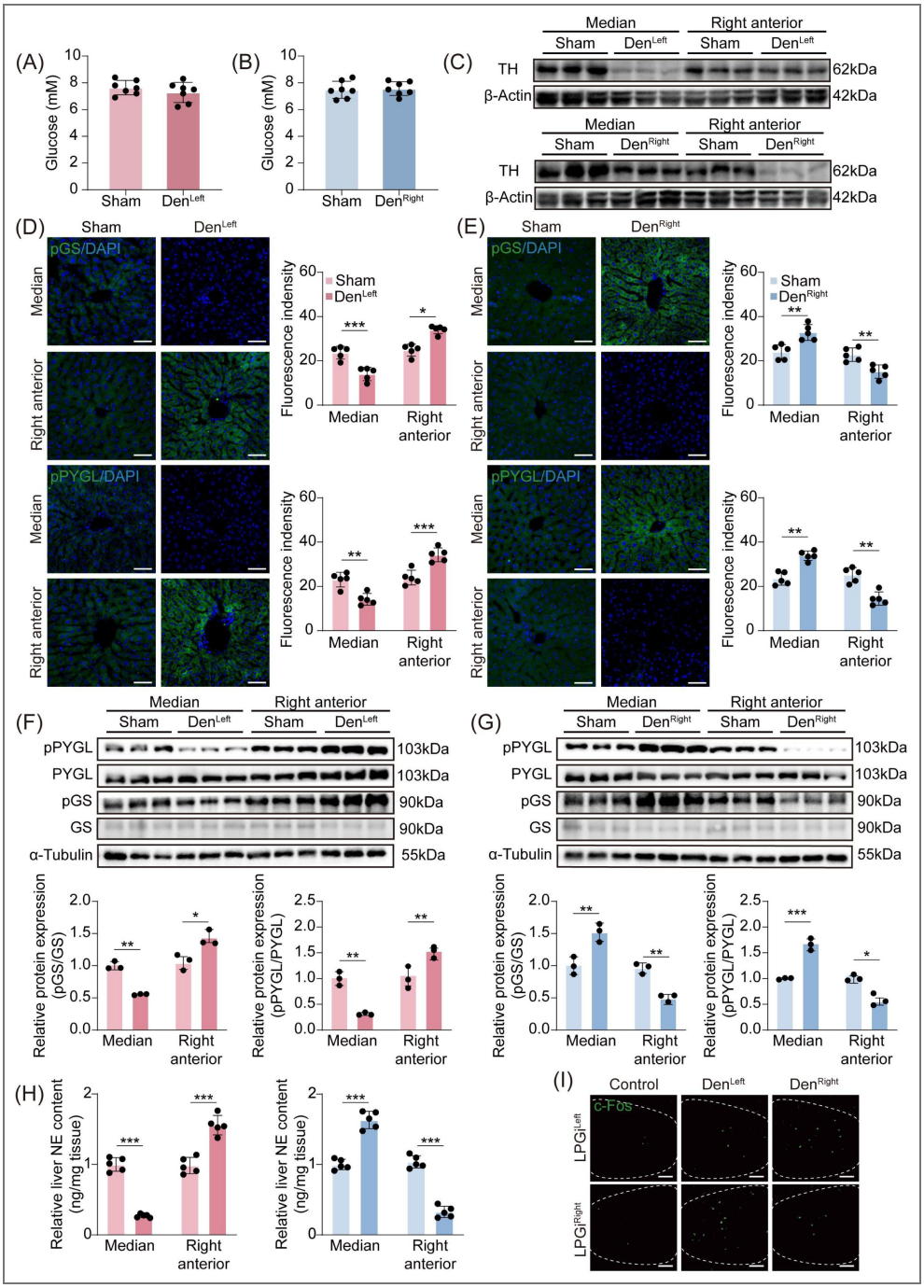

Figure 3. LPGi maintains glucose balance through compensatory use of ipsilateral hepatic lobes under contralateral lobe impairment.

(A and B) Blood glucose levels in the left- (A, n = 7) or right-sided (B, n = 7) lobes denervated mice. (C) Western blot of TH protein in median and right anterior lobes after denervating left- (top) or right-sided (bottom) lobes (n = 3). (D and E) Representative immunofluorescence images of pGS (top) and pPYGL (bottom) expression in right anterior and median lobes in left- (D) or right-sided (E) lobes denervated mice, with quantification of relative fluorescence intensity (right, n = 5). Scale bars, 100 μm. (F and G) Western blot analysis of pPYGL, PYGL, pGS, and GS proteins in median and right anterior lobes (top) in left- or right-sided lobes denervated mice, with densitometric quantification (bottom, n = 3). (H) NE contents of median and right anterior lobes in left- or right-sided lobes denervated mice (n = 6). (I) Representative immunofluorescence images of c-FOS expression in left and right LPGi in left- or right-sided lobes denervated mice. Scale bars, 100 μm. Data are presented as means ± SEM, with individual values shown for all experiments. *p < 0.05, **p < 0.01, ***p < 0.001. Unpaired Student's t-test for (A-B, D-H)

unknown. Using whole-mount clearing, we visualized the brain–liver sympathetic circuit and found that preganglionic neurons in the spinal cord send descending fibers through the sympathetic chain (SyC) to innervate postganglionic neurons in the CG-SMG (Figure 4A). Further whole-mount TH immunostaining showed that TH-positive sympathetic cell bodies within the CG-SMG project to the liver along the hepatic vasculature (Figure 4B and Figure S5F). These observations suggest that the nerve bundles likely decussate at the porta hepatis before entering the individual hepatic lobes.

To test this, we performed unilateral anterograde tracing by injecting AAV-TH-DIO-EGFP into a single CG (Figure S5G). This revealed a strictly contralateral innervation pattern: the left CG mainly projected to the right posterior, right anterior, and caudate lobes, whereas the right CG prominently innervated the left lateral and median lobes (Figure 4C). To validate this pattern, we performed dual retrograde tracing by injecting Alexa Fluor 647- and 555-conjugated wheat germ agglutinin (WGA) into left- and right-sided lobes, respectively (Figure S5H). Consistent with the anterograde results, left CG neurons predominantly projected to the right-sided lobes, while right CG neurons targeted the left-sided lobes, confirming robust contralateral preference (Figure 4D). Thus, these findings demonstrate that central inputs descend via the SyC to the CG-SMG complex, where nerve bundles converge and extend along the portal vein, branching within the porta hepatis to innervate individual hepatic lobes.

To explore the development of the intrahepatic neural network in mice, we therefore performed tissue clearing on the torsos of mice from postnatal weeks 0 to 2. We observed that at week 0, the sympathetic nerve bundles were located at the porta hepatis but had not yet extended into the liver (Figure 4E, left). By week 1, the sympathetic nerves had begun to grow into the liver (Figure 4E, middle). It was not until week 2 that the sympathetic nerves fully infiltrated all liver lobes (Figure 4E, right). These findings indicate that, after the first postnatal week, sympathetic nerves grow from the porta hepatis into the liver lobes and form a well-developed sympathetic neural network by the second week.

Discussion

The CNS exhibits functional asymmetry despite structural bilateral symmetry, a phenomenon well recognized in language, handedness, and spatial cognition.[32,33] Recent advances extend this concept beyond cortical domains to central autonomic regulation of peripheral organs.[34,35] Trans-neuronal tracing of symmetrical organs such as the kidneys and thymus has revealed contralateral control with bilateral coordination,[8,35] whereas the lateralized regulation of asymmetrical organs like the liver, heart, and stomach remains poorly defined and conflicting.[6,12,37] For instance, parasympathetic cardiac control has been reported to exhibit left-hemispheric dominance,[6] yet clinical evidence revealed that arrhythmias may arise after strokes in either hemisphere.[38] These discrepancies highlight the complexity of lateralized autonomic control and the intrinsic bilaterality within the autonomic network. In this study, we systematically mapped and functionally interrogated the laterality of brain-liver circuitry, focusing on the LPGi. Our anatomical and functional experiments provide compelling evidence that although a subset of LPGi neurons project bilaterally, the predominant organization is contralateral and lobe-specific.

Recent advances in viral tracing and whole-tissue imaging have greatly accelerated our understanding of peripheral neuroanatomy.[39–41] For instance, distinct gastrointestinal regions are differentially regulated by subdivisions within the CG-SMG,[19] while the kidneys predominantly receive ipsilateral input from sympathetic postganglionic neurons residing in the renal sympathetic ganglia.[20] In contrast, components of the immune system, such as the thymus, exhibit lateralized central regulation, with each hemisphere preferentially modulating the contralateral thymic lobe.[36] Using PRV-mediated retrograde tracing with whole-mount clearing, we mapped a brain-liver axis arising from the LPGi and revealed a strikingly lateralized projection pattern: left LPGi neurons preferentially innervated right-sided lobes, whereas right LPGi neurons predominantly targeted left-sided lobes. A small subset of LPGi neurons was double-labeled after bilateral PRV injections, suggesting a fraction of these neurons projects bilaterally to both sides of

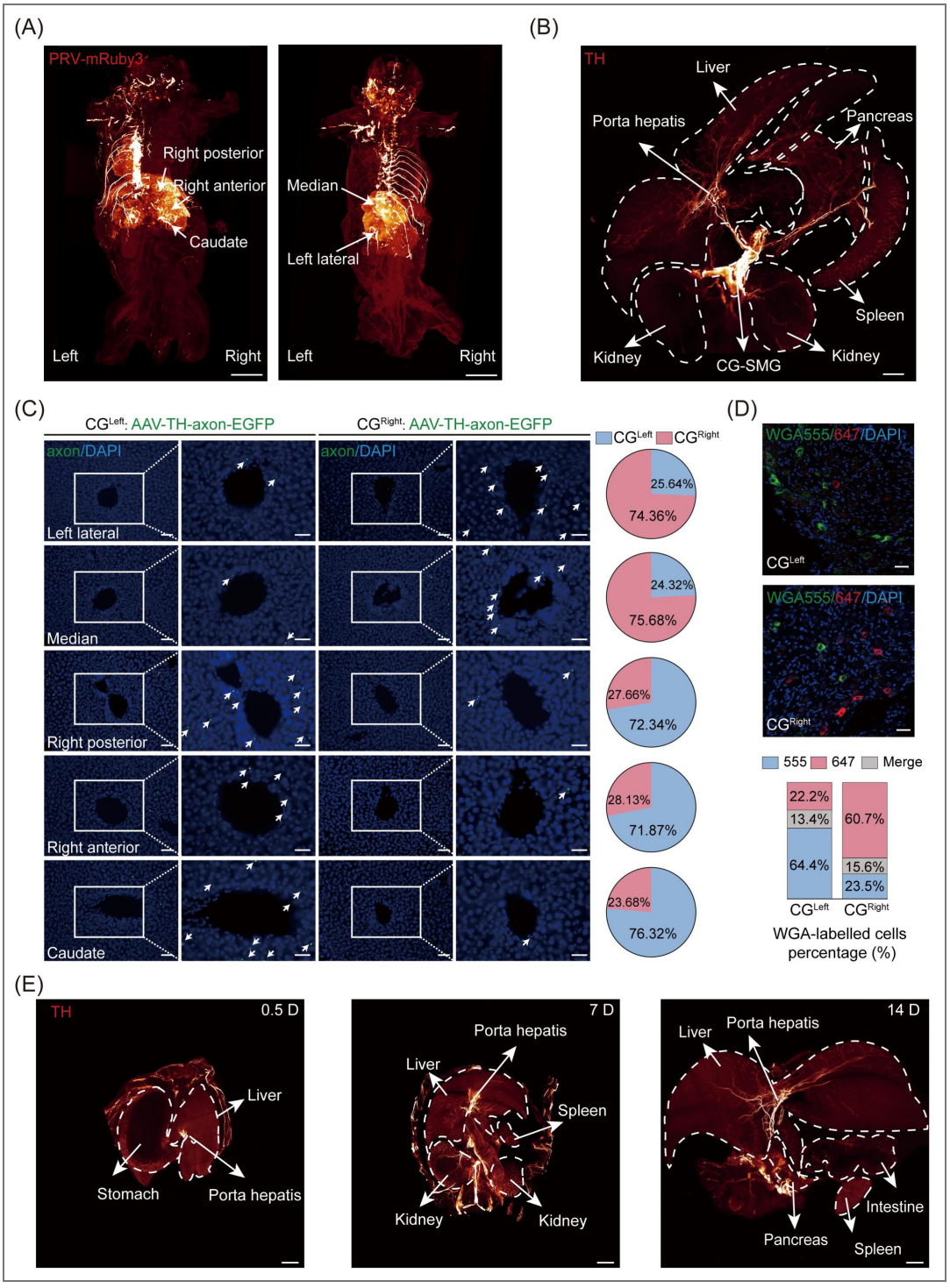

Figure 4. Sympathetic projections to the liver decussate at the porta hepatis, progressively formed during development.

(A) Representative 3D images of mice following PRV injection into right- (left) or left-sided (right) lobes. Scale bars, 3000 μm. (B) Representative 3D images of CG-SMG projections to peripheral organs. Scale bar, 3,000 μm. (C) Representative images of sympathetic axons after unilateral CG injection, with quantification of EGFP-labeled axon distribution across hepatic lobes. Scale bars, 100 μm. (D) Representative images of WGA-labeled neurons in left and right CG, with percentages of WGA555^{+}, WGA647^{+}, and co-labeled neurons. Scale bars, 100 μm. (E) Representative images showing the developmental progression of CG-SMG projections to the liver from postnatal week 0 to week 2. Scale bars, 3,000 μm.

the liver. Such neurons may support interlobar coordination. Together, this high-resolution anatomical mapping provides direct evidence for lateralized central projections to an asymmetric organ and reveals a previously unrecognized dimension of laterality in autonomic liver innervation.

Functionally, this anatomical organization translates into lobe-specific regulation of HGP. Sympathetic innervation of the liver is well established as a major driver of glucose output, with prior electrical stimulation studies demonstrating robust hepatic glucose release in response to sympathetic activation.[42–44] Consistent with these observations, both chemogenetic and optogenetic activation of LPGi GABAergic neurons significantly elevated systemic glucose levels by promoting glycogenolysis and gluconeogenesis in the contralateral lobes. These metabolic responses were accompanied by localized NE release, increased phosphorylation of key metabolic enzymes (pPYGL and pGS), and glycogen depletion.[45,46] Bilateral LPGi activation produced additive effects, indicating that both sides of the brainstem can cooperatively regulate hepatic metabolism in a spatially segregated manner. This pattern suggests that hepatic glucose output can be modulated in a lobe-specific, rather than uniform whole-organ, manner. This spatial organization is likely obscured by conventional electrical stimulation, which indiscriminately activates heterogeneous sympathetic fibers.[44,45] By contrast, chemogenetic and optogenetic approaches permit selective, cell type-specific manipulation of LPGi neurons, thereby revealing the contralateral and lobe-specific architecture of brain-liver sympathetic control.

Beyond identifying lateralized control, we also reported a compensatory mechanism following unilateral hepatic denervation. When neural input from one side of the brainstem was attenuated, compensatory neural plasticity emerged through increased sympathetic drive from contralateral LPGi, enhancing gluconeogenesis and glycogenolysis within the remaining innervated hepatic lobes. This response was supported by increased c-FOS expression in contralateral LPGi, higher intrahepatic NE content, and elevated pPYGL and pGS expression in unaffected lobes. Such plasticity parallels compensatory phenomena in other systems, including contralateral enhancement after renal dysfunction and cortical dominance shifts in patients with unilateral hearing loss.[26,47] Although enhanced sympathetic output appears to mediate much of this compensation, our findings suggest that the underlying regulation extends beyond a purely descending pathway. In particular, c-FOS activation in the contralateral LPGi after unilateral 6-OHDA-mediated denervation suggests that the loss of peripheral input may be sensed through an ascending neural pathway, centrally integrated, and translated into compensatory sympathetic output to the intact hepatic lobes. These results therefore support a model in which hepatic glucose production is regulated by an integrated afferent-central-efferent loop, with our current analyses primarily resolving its efferent component.

We further show that contralateral regulation of hepatic metabolism arises from a peripheral decussation, challenging the long-held view that such organization arises exclusively from central crossings. Unlike somatic and sensory systems, where contralateral control is mediated by pyramidal or optic decussations in CNS nuclei,[2,28,29] hepatic sympathetic projections descend ipsilaterally from the brainstem to the CG-SMG before crossing to innervate contralateral lobes. This peripheral arrangement suggests that spatially organized control can be implemented downstream of peripheral ganglia, representing a potential evolutionary adaptation. More broadly, it calls for re-examination of neural laterality paradigms and identifies peripheral ganglia as decision nodes and therapeutic targets for organ-specific neuromodulation.

Despite these advances, several limitations warrant mention. First, the neuronal subtypes within the LPGi that mediate contralateral projections remain unidentified. Future research combining genetic labeling with single-cell RNA sequencing will be needed to resolve their molecular and functional identities. Second, technical constraints prevented simultaneous bilateral viral tracing and whole-mount mouse imaging in the same animal, restricting direct assessment of interhemispheric interactions. Third, although whole-mount TH immunostaining with three-dimensional reconstruction revealed sympathetic nerve bundles projecting from the CG to the liver, TH is not entirely specific and can also label a subset of sensory neurons. More selective approaches, such as genetic targeting of sympathetic lineages, will be important for further

validation. Fourth, although our data support a peripheral decussation at the porta hepatis, direct validation of this crossover site was not feasible with local pharmacological blockade, as currently available approaches lack sufficient spatial specificity and would likely perturb multiple neural components. Future studies employing more selective inhibitory strategies will be required to directly test this possibility. Finally, although our murine data provide new insights into lateralized autonomic control of hepatic metabolism, their translational relevance to humans remains to be established. Progress in noninvasive imaging and neural circuit mapping may ultimately enable analogous studies in clinical settings.

In conclusion, this study establishes that the brain exerts lateralized and lobe-specific control over hepatic glucose metabolism, with contralateral regulation arising from a peripheral decussation at the porta hepatis, and a compensatory mechanism maintaining glucose homeostasis after unilateral hepatic injury. Developmentally, sympathetic projections began extending into the liver during the first postnatal week, forming a mature network by week 2 that enables both baseline regulation and adaptive responses. Together, these findings extend the concept of lateralization beyond cognition, motor control, and symmetric organs, with potential implications for targeted neuromodulation strategies in organ-specific diseases.

Methods

Animals

All animal experiments were performed in accordance with the Guide for the Care and Use of Laboratory Animals and were approved by the Institutional Animal Care and Use Committee of China Pharmaceutical University. Adult C57BL/6J mice (male, 8-week-old) were used in this study. Mice were group-housed (3-5 per cage) under a standard 12-hour light/dark cycle (lights on at 7:00 AM) at a controlled temperature (22 ± 1 °C) and humidity (50 ± 10%), with ad libitum access to a standard laboratory chow diet and water. For all surgical and terminal procedures, mice were anesthetized with isoflurane (induction 3-4%, maintenance 1.5-2% in 100% oxygen). Littermates of the same sex were randomly assigned to experimental or control groups using a random number generator. Experimenters were blinded to group allocation during data collection and analysis where feasible. All efforts were made to minimize animal suffering and to use the minimum number of animals required for statistical reliability.

Viral vectors

For retrograde tracing of LPGi projection to individual hepatic lobes, we injected PRV-CAG-EGFP (BrainVTA, Cat#P03001) and PRV-CAG-mRFP (BrainVTA, Cat#P03002) into distinct hepatic lobes, respectively. For chemogenetic manipulation, we used a combination of AAV9-GAD67-Cre (BrainVTA, Cat#PT-6600) with AAV9-DIO-hM3Dq (BrainVTA, Cat#PT-0019) or AAV9-DIO-mCherry (BrainVTA, Cat#PT-0115). For optogenetic manipulation, we used a combination of AAV9-GAD67-Cre with AAV9-DIO-ChR2-mCherry (BrainVTA, Cat#PT-0002) or AAV9-DIO-mCherry. For anterograde tracing from the CG-SMG to hepatic lobes, we injected AAV9-TH-Cre (BrainVTA, Cat#PT-2947) with AAV9-EF1α-DIO-Axon-EGFP (BrainVTA, Cat#BC-0197) into the unilateral CG-SMG. All viral vectors were used at titers $<5 \times 10^{12}$ vg/mL.

PRV injection

For retrograde tracing from the liver, pseudorabies virus (PRV-CAG-EGFP, 5.00×10^{9} PFU/ml, BrainVTA, Cat#P03001) was used to identify upstream autonomic inputs to the hepatic lobes. Following laparotomy and exposure of the liver as described above, a series of focal injections was performed to restrict viral labeling to circuit-specific connections. A total volume of 1 μL of PRV per lobe was slowly pressure-injected into the targeted lobe using a glass micropipette attached to a microsyringe. Injections were made at multiple sites (2-3 sites) within each lobe, with careful coordination to avoid leakage into the peritoneal cavity or surrounding tissues. Following each injection, the micropipette was left in place for 5 min to minimize backflow, and the injection site

was briefly swabbed with sterile saline. The intestines were then repositioned, and the abdominal wall was sutured. Animals were perfused 5 days post-injection, and brain sections were processed for PRV immunodetection to map infected neuronal populations.

Quantification of PRV-labeled neurons

For quantitative analysis, serial coronal sections (40 μm thickness) encompassing the entire rostrocaudal extent of the LPGi were collected. Every third section was selected for immunostaining and imaging. Images were captured using a fluorescence microscope (Leica) with a 20×objective. PRV-positive neurons in each selected section were counted manually using the Cell Counter plugin in ImageJ software. Neurons were identified based on fluorescent signal intensity above background and characteristic neuronal morphology with clearly labeled nuclei and cytoplasm.

Brain stereotactic injection

Mice were anesthetized with isoflurane (RWD Life Science Co., Ltd., Cat#68811). For brain injection, the coordinates of LPGi were determined using the Allen Mouse Brain Atlas (AP−6.75 mm, ML ±0.95 mm, DV −5.85 mm). A total of 200 nL of viral vector was bilaterally delivered at a rate of 50 nL/min.

Intrahepatic sympathetic nerve tracing

Following laparotomy, the intestines were gently exteriorized and covered with saline-moistened gauze to expose the celiac ganglion-superior mesenteric ganglion (CG-SMG). For anterograde tracing of CG-SMG projections to hepatic lobes, a viral cocktail containing AAV9-TH-Cre (BrainVTA, Cat#PT-2947) and AAV9-EF1 α-DIO-Axon-EGFP (BrainVTA, Cat#BC-0197) was injected into either the left or right CG using fine glass micropipettes. A volume of 100 nL per site was delivered at a slow infusion rate of 50 nL/min to minimize tissue damage and restrict viral spread to the targeted ganglion, and tissues were collected 3 weeks post-injection. For retrograde tracing, 500 nL of 1 mg/ml Alexa Fluor 647-conjugated wheat germ agglutinin (WGA 647, Thermo, Cat#W32466) and Alexa Fluor 555-conjugated wheat germ agglutinin (WGA 555, Thermo, Cat#W32464) were injected into the left- and right-sided lobes, respectively, using an infusion rate of 100 nL/min. Tissues were harvested 3 days thereafter.

Intrahepatic sympathetic denervation

To achieve lobe-specific sympathetic denervation, individual hepatic lobes were physically separated and isolated during the injection procedure to minimize diffusion of the neurotoxin to adjacent tissue. The injection volume was calculated based on the proportion of each lobe relative to the total liver weight. A solution of 6-hydroxydopamine (6-OHDA, 12 mg/ml in sterile saline containing 0.01% ascorbic acid; Sigma, Cat#162957) was injected into each target lobe at a volume of 2,500-3500 nL and a flow rate of 300 nL/min.

Whole-mount clearing and imaging

The liver and trunk staining procedure was performed according to established protocols as previously described.[14,48] In brief, the liver tissues were fixed in 4% paraformaldehyde (PFA), followed by permeabilization in PBS containing 0.2% Triton X-100, 20% DMSO, and 0.3 M glycine. Immunostaining was performed using the primary antibody against TH (Merck, Cat #AB152, 1:500), followed by incubation with a secondary antibody (Alexa Fluor 568-conjugated donkey anti-rabbit IgG, Thermo Fisher, Cat#A-10042). After staining, tissues were embedded in 1% agarose, dehydrated, and cleared using dibenzyl ether (DBE; Sigma, Cat#422053).

The brain-liver neurocircuit visualization was performed as previously described.[25] At 5 days post-injection of PRV, the mice were anesthetized with isoflurane and perfused with PBS. Samples were permeabilized in PBS containing 1.5% goat serum, 0.5% Triton X-100, 0.5 mM methyl-β-cyclodextrin, and 0.2% trans-1-acetyl-4-hydroxy-l-proline. Following permeabilization, samples were stained with mRuby3 nanobody (NanoTag, Cat#N3302-AF647-L, 1:5,000). They were then

dehydrated with upgraded tetrahydrofuran (THF; Sigma, Cat#401757), and subsequently incubated in dichloromethane (Sigma, Cat#270997). Finally, samples were cleared by benzyl alcohol and benzyl benzoate mixture (Sigma, Cats #24122 and #W213802).

The cleared samples were imaged using a light-sheet fluorescence microscope (Nuohai, LS18) at 1.25×, 3.2×, and 12.6× magnification. Finally, full-tissue image stacks were reconstructed and analyzed using Imaris ×64 software (version 9.5.0, Bitplane).

Chemogenetic and optogenetic manipulations

For chemogenetic manipulation, we stereotaxically injected mice with 200 nL of AAV carrying the Cre-dependent activator DREADD (AAV9-DIO-hM3Dq-mCherry) and allowed them to recover for at least four weeks before conducting tests.

For optogenetic manipulation, mice received stereotaxic injections of 200 nL AAV9-DIO-ChR2-mCherry into the LPGi, followed by implantation of optical fibers (Inper, Cat#D3429). After a four-week recovery, mice were habituated to a fiber-optic patch cord in the home cage for 2 hours before the stimulation. Blue light (465 nm) stimulation, consisting of pulse trains (10 ms pulses of 20 Hz at approximately 10 mW; 1 s on, 1 s off), was delivered.

Biochemical assays

The concentrations of epinephrine (EPI), norepinephrine (NE), insulin (INS) and glucagon (GC) were quantified using the EPI enzyme-linked immunosorbent assay (ELISA) kit (Kexing, Cat#Fankew F2351-A), NE ELISA kit (Kexing, Cat#Fankew F2533-A), INS ELISA kit (Kexing, Cat#Fankew F2579-A) and GC ELISA kit (Kexing, Cat#Fankew F2167-A). PEPCK activity assay kit (Kexing, Cat#Fankew F2533) and G6PC activity assay kit (Kexing, Cat#Fankew F2736-A) were used to quantify the activity of phosphoenolpyruvate carboxykinase (PEPCK) and glucose-6-phosphatase (G6PC).

Western blot analysis

Tissue samples were homogenized in RIPA lysis buffer (Beyotime, Cat#P0013B) with 100 μM protease and phosphate inhibitors (Beyotime, Cat#P1045) using a homogenizer (JieChen Instrument, JCZYM-48R) at 4 °C. The following primary antibodies were used: PEPCK (Santa, Cat#sc-271029, 1:1,000), G6PC (Novus, Cat#NBP1-80533, 1:1,000), pPYGL (Ser15) (Abcam, Cat#ab227043, 1:1,000), PYGL (Proteintech, Cat#15851-1-AP, 1:1,000), pGS (Ser641) (Cell Signaling Technology, Cat#3891S, 1:1,000), GS (Santa, Cat#sc-81173, 1:1,000), TH (Merck, Cat#AB152, 1:1,000), and α-Tubulin (Huabio, Cat#ER130905, 1:10,000), followed by incubation with appropriate secondary antibodies. Imaging of membranes was performed with the iBright Imaging Systems (Thermo, iBright 1500). We quantified the signal intensities by performing densitometric analyses using Fiji (ImageJ, NIH).

Histology and immunofluorescence analyses

Mouse livers and brains were collected separately and fixed with 4% PFA overnight at 4 °C. For Periodic Acid-Schiff (PAS) staining, 25 μm paraffin sections were prepared and stained with a PAS staining kit (Beyotime, Cat#C0142S). For immunostaining, 25-μm-thick frozen sections were prepared by a freezing microtome (Leica, CM 1950) and stained with primary antibodies, including anti-c-FOS (Synaptic Systems, Cat#226-008, 1:1,000), anti-TH (Merck, Cat#AB152, 1:500), anti-pPYGL (Ser15) (Abcam, Cat#ab227043, 1:100), and anti-pGS (Ser641) (Cell Signaling Technology, Cat#3891S, 1:100), followed by incubation with secondary antibody (Alexa Fluor 488-conjugated goat anti-rabbit IgG, Yeasen, Cat#33116ES60). The sections were imaged using confocal microscopes (Zeiss, LSM 700). Images were quantified with ImageJ (v1.8.0).

Quantification and statistical analysis

An unpaired two-tailed Student's t-test was used to compare differences between two groups. Comparisons across multiple groups were conducted using one-way ANOVA with the Tukey test. All results, including graphs, were expressed as means ± SEM unless otherwise specified. Significance was defined as $p < 0.05$, with significance annotations of * $p < 0.05$, ** $p < 0.01$, *** $p < 0.001$; $^{\#}$ $p < 0.05$, $^{\#\#}$ $p < 0.01$, $^{\#\#\#}$ $p < 0.001$; $^{\$}$ $p < 0.05$, $^{\$\$}$ $p < 0.01$, $^{\$\$\$}$ $p < 0.001$. Statistical analyses were conducted using software such as GraphPad Prism (v.10.0), ImageJ (v1.8.0), and syglass (2.4.0).

Data availability

All data generated or analyzed during this study are included in themanuscript and supporting files. Source data files have been provided for all figures.

Supplementary figures

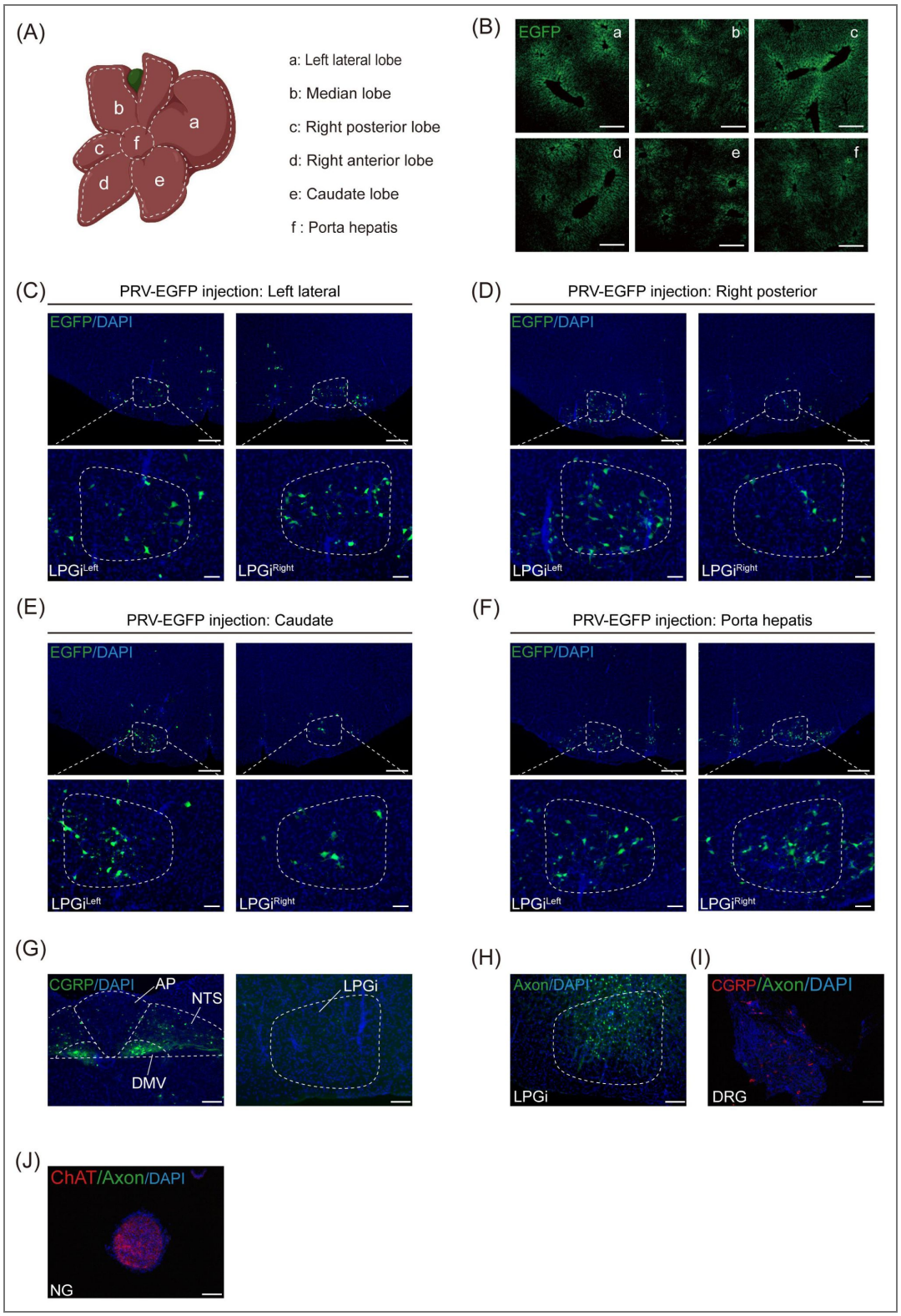

Supplementary figure 1. Supplementary evidence for contralateral projections from the brain to the liver, related to Figure 1. (A) Schematic illustration of hepatic lobes with anatomical labeling. (B) Representative images of hepatic lobes after PRV-EGFP injections. Scale bars, 150 μm. (C) (C-F) Representative immunofluorescence images of PRV-labeled neurons (EGFP) in the left and right LPGi following PRV injections into left lateral lobe (C), right posterior lobe (D), caudate lobe (E), and porta hepatis (F). Scale bars, 200 μm (top) and

100 μm (bottom). (G) Representative immunofluorescence images showing CGRP (green) and DAPI (blue) in NTS(left) and LPGi (right). Scale bar, 100 μm (H) Representative immunofluorescence images of Axon.-EGFP^{+} neuron in LPGi. Scale bar, 100 μm (I) Representative immunofluorescence images showing CGRP (red), Axon-EGFP labeling (green)and DAPI (blue) in DRG. Scale bar, 100 μm (j) Representative immunofluorescence images showing choline acetyltransferase (ChAT, red),Axon-EGFP labeling (green) and DAPI (blue) inNG. Scale bar, 100 μm

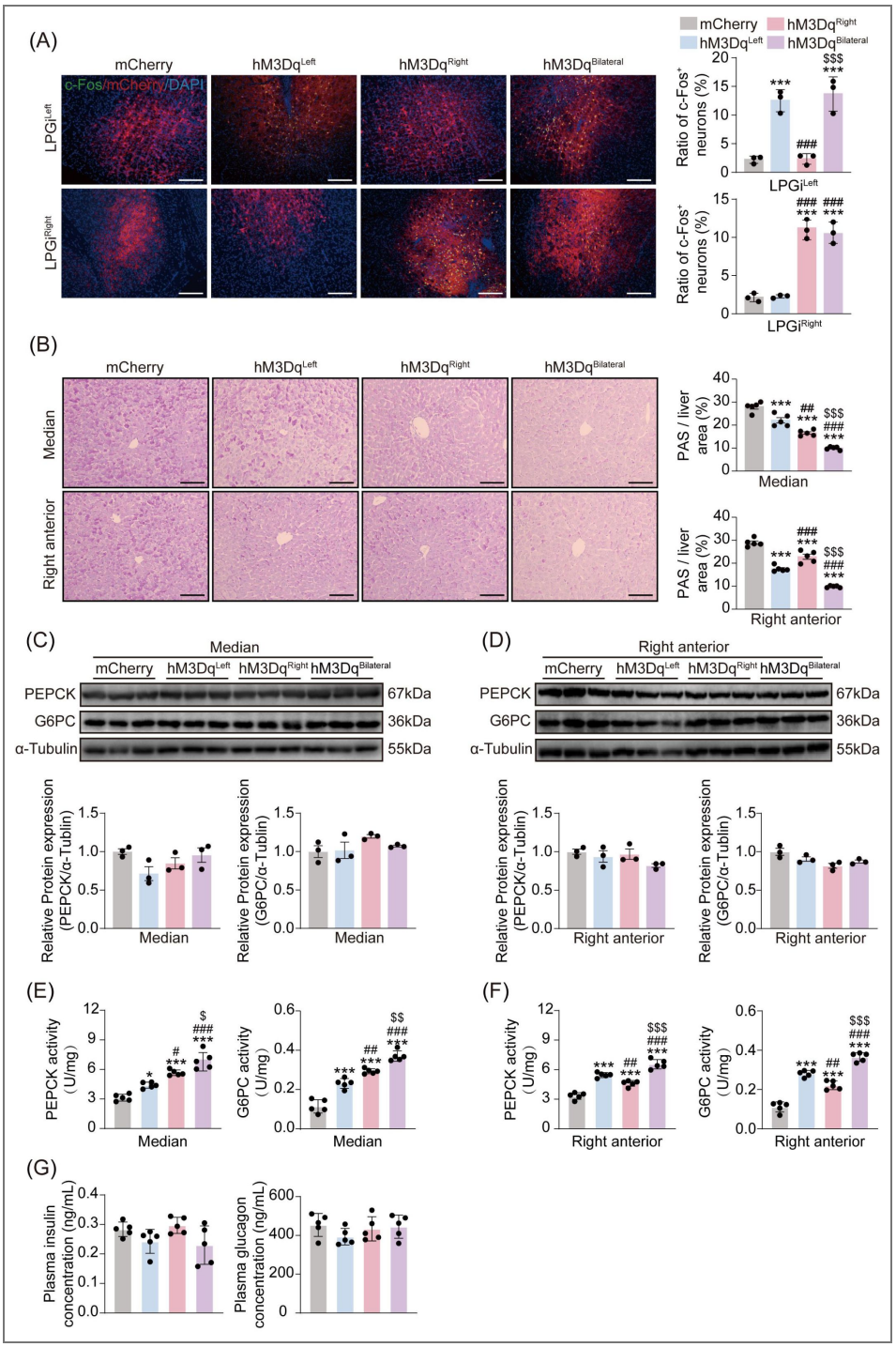

Supplementary figure 2. Chemogenetic activation of LPGi induces c-Fos expression, promotes hepatic glycogenolysis, and activates glycogenolytic enzymes, related to

Figure 2. (A) Representative immunofluorescence images of c-FOS^{+} LPGi neurons in hM3Dq mice following 1 h stimulation (Left), with quantification ofc-FOS^{+} neuron percentage (right, *n* = 3). Scale bars, 100 μm. (B) Representative PAS staining images of median (top) and right anterior (bottom) lobes in hM3Dq mice following 1 h stimulation, with semi-quantitative analysis of glycogen levels (right, *n* = 5). Scale bars, 100 μm. (C and D) Western blot analysis of PEPCK and G6PC proteins in the median (C, top) and right anterior (D, top) lobes, with densitometric quantified (bottom, *n* = 3). (E and F) Enzyme activity ofPEPCK and G6PC in the median (E) and right anterior (F) lobes (*n* = 3). (G) Plasma concentrations of insulin (Left, n = 5) and glucagon (Right, n = 5) GAD^{mCherry} and GAD^{hM3Dq} mice following 1h. Data are expressed as means ± SEM, with individual values shown for all experiments. *$p < 0.05$, *** $p < 0.001$; $^{\#\#}$ $p < 0.01$, $^{\#\#\#}$ $p < 0.001$; $^{\$\$\$}$ $p < 0.001$. A one-way ANOVA with the Tukey test was used for (A-F).

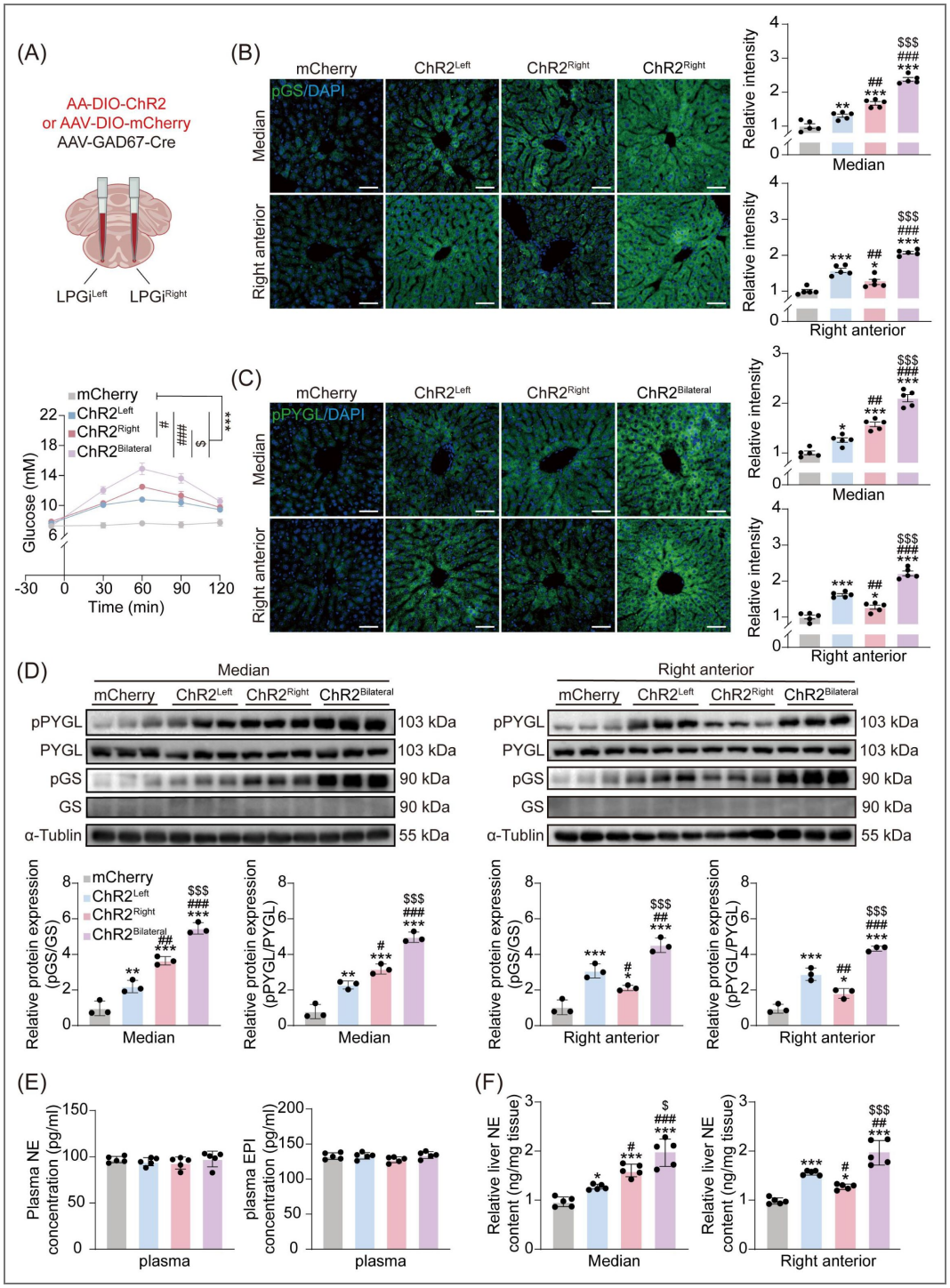

Supplementary figure 3. Optogenetic activation of LPGi confirms contralateral lobe-specific mobilization observed in

Figure 2. (A) Scheme for injecting AAV-DIO-ChR2 or AAV-DIO-mCherry (top). Blood glucose levels following optogenetic activation of left, right, or bilateral LPGi, measured at −10, 30, 60, 90, and 120 min (bottom, $n = 6$) (B and C) Representative immunofluorescence images of pGS (B) and pPYGL (C) expression in median (top) and right anterior (bottom) lobes after 1 h optogenetic activation of left, right, or bilateral LPGi, with quantification of relative fluorescence intensity ($n = 5$). Scale bars, 100 μm. (D) Western blot analysis of pPYGL, PYGL, pGS, and GS in median (left) and right anterior (right) lobes after 1 h activation, with densitometric quantification (bottom, $n = 3$). (E) Plasma concentrations of norepinephrine (NE) (left, $n = 5$) and epinephrine (EPI) (right, $n = 5$) following 1 h optogenetic activation. (F) NE contents in median (left, $n = 5$) and right anterior (right, $n = 5$) lobes after 1 h optogenetic activation. Data are expressed as means ± SEM, with individual values shown for all experiments. * $p < 0.05$, ** $p < 0.01$, *** $p < 0.001$; # $p < 0.05$, ## $p < 0.01$, ### $p < 0.001$; $ $p < 0.05$, $$$ $p < 0.001$. A one-way ANOVA with the Tukey test was used for (A-F).

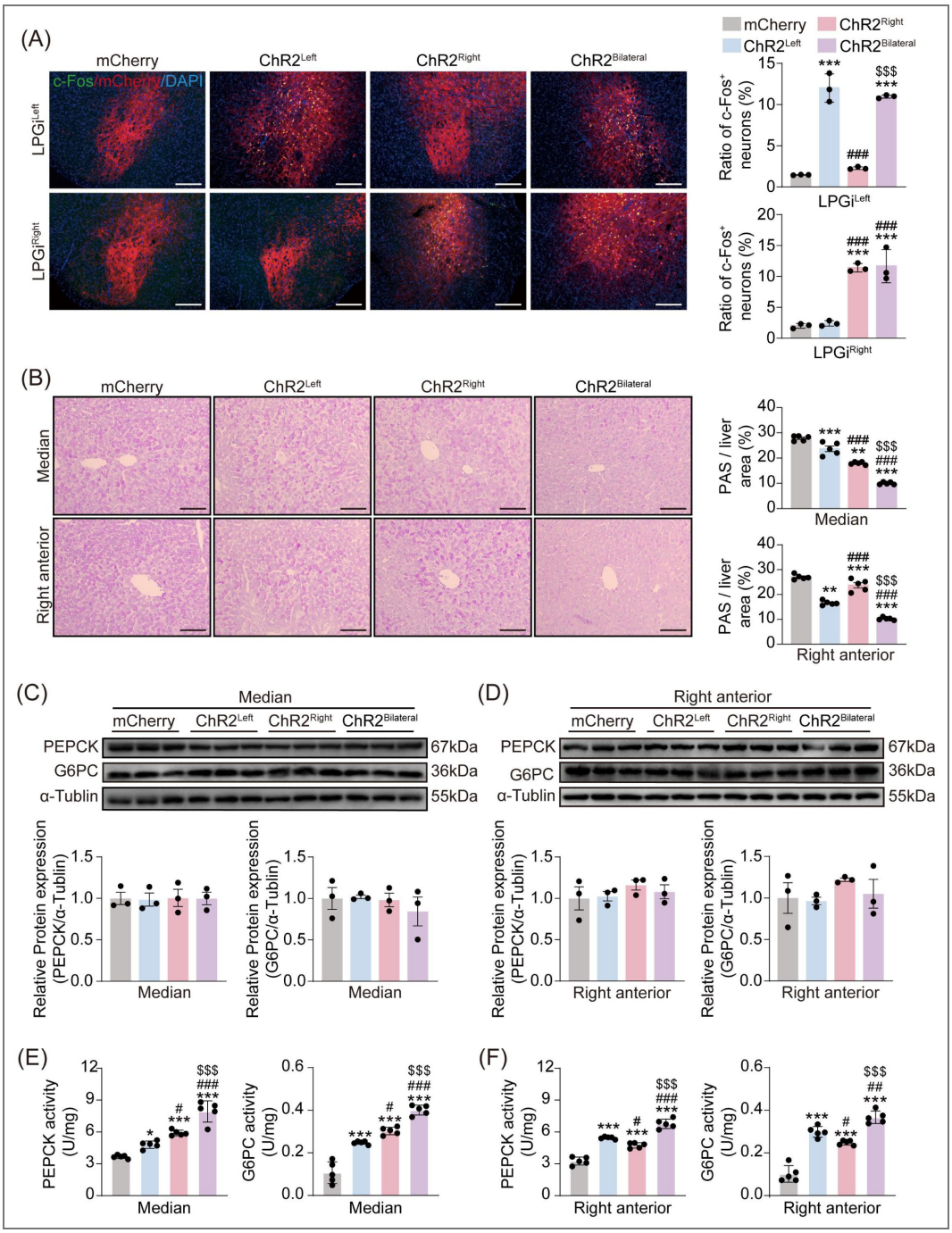

Supplementary figure 4. Optogenetic activation of LPGi recapitulates c-Fos expression, hepatic glycogenolysis, and activity of glycogenolysis-related enzymes observed in Figure S2.

(A) Representative immunofluorescence images of c-FOS^{+} neurons in LPGi after 1 h optogenetic stimulation, with quantification of ratio of c-FOS^{+} neurons (right, n = 3). Scale bars, 100 μm. (B) Representative PAS staining images of the median (top) and right anterior lobes (bottom) lobes following 1 h optogenetic stimulation, with semi-quantitative analysis of glycogen levels (n = 5). Scale bars, 100 μm. (C and D) Western blot analysis of PEPCK and G6PC proteins in median (C) and right anterior(D) lobes, with densitometric quantification (n = 3). (E and F) Enzyme activity of PEPCK and G6PC in median (E) and right anterior lobes (F) (n = 3). Data are expressed as means ± SEM, with individual values shown for all experiments. * p < 0.05, ** p < 0.01, *** p < 0.001; $^{\#}$ p < 0.05, $^{\#\#}$ p < 0.01, $^{\#\#\#}$ p < 0.001; $^{\$\$\$}$ p < 0.001. A one-way ANOVA with the Tukey test was used for (A-F).

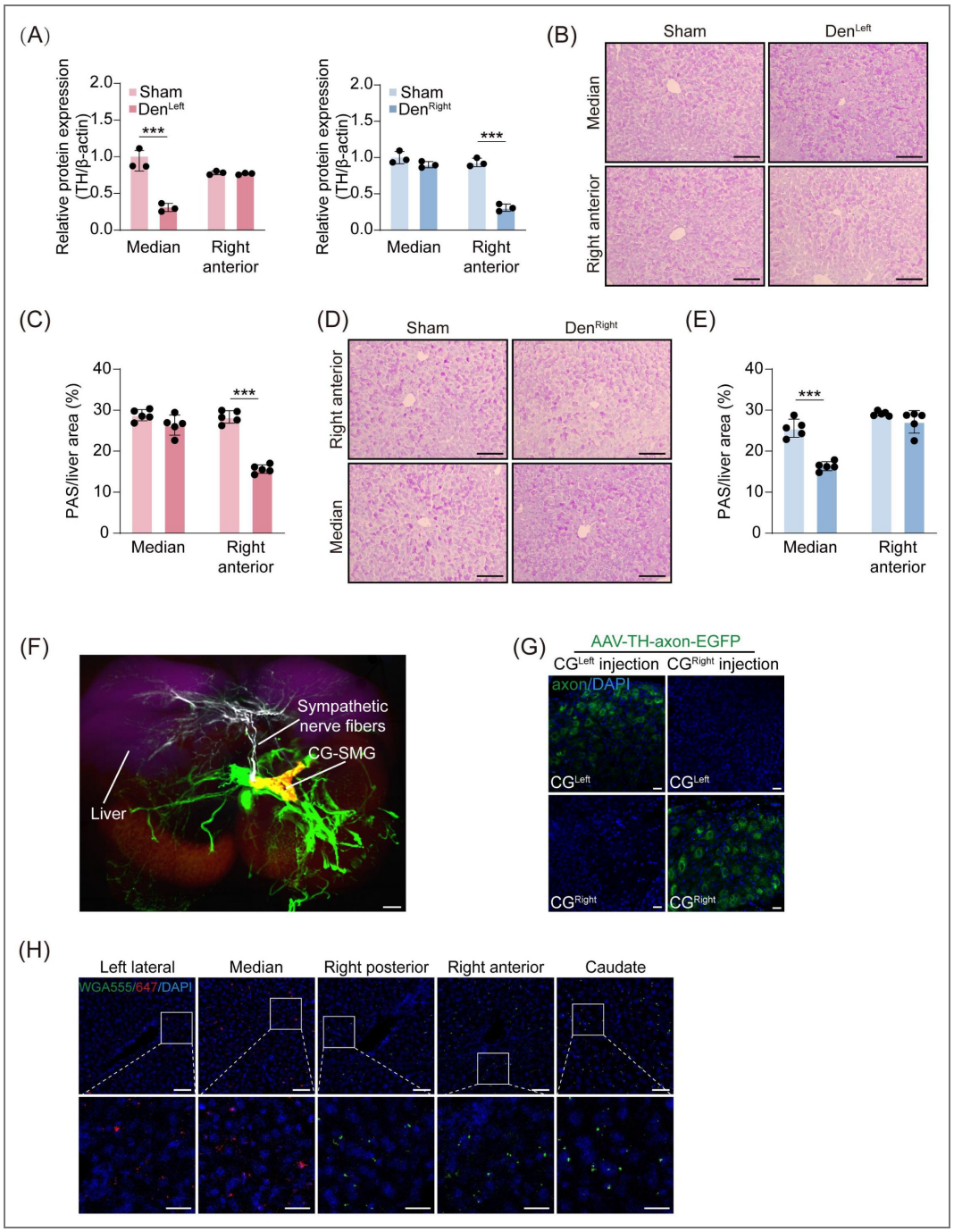

Supplementary figure 5. Validation of sympathetic nerve ablation, enhanced glycogenolysis in non-denervated hepatic lobes, and accurate targeting of AAV and WGA injections, related to Figure 3 and 4.

(A) Densitometric quantification of TH protein in median and right anterior lobes after denervating left- (left) or right-sided (right) lobes. (B-E) Representative PAS staining images of median (top) and right anterior (bottom) lobes in left- (B) and right-sided (D) lobes denervated mice, with semi-quantitative analysis of glycogen levels (C and E, $n = 5$). Scale bars, 100 μm. (F) Representative 3D images of CG-SMG projections to peripheral organs (liver, purple; sympathetic nerve fibers, white; CG-SMG, yellow; TH-positive nerve fibers, green). Scale bar, 3,000 μm. (G) Represent slices of the CG in unilateral AAV-TH-axon-EGFP injected mice. Scale bars, 20 μm. (H) Represent slices of hepatic lobes after injecting WGA 647 and WGA 555 into left-and right-sided lobes. Scale bars, 50 μm. Data are expressed as means ± SEM, with individual values shown for all experiments. *** $p < 0.001$; Unpaired Student's t-test for (A, C, and E).

Acknowledgements

We thank the following agencies for financial support: the National Natural Science Foundation of China (82301436, 82371311, 81930109, and 82321005), National Key R&D Program of China (2021YFA1301300, 2023YFA1801900); the Natural Science Foundation of Jiangsu Province (BK20221050, BG2024045), the Overseas Expertise Introduction Project for Discipline Innovation (G20582017001), the Jiangsu Specially Appointed Professor Program, and the International Postdoctoral Talent Recruitment Program, the Postgraduate Research & Practice Innovation Program of Jiangsu Province (KYCX25_1076).

Additional information

Author contribution

H.X., H.H., and X.Z. conceived, designed, and supervised the project. Z.W., M.R., Y.C., and Y.L. performed glucose level monitoring and data analysis. X.G., K.W., Y.C., and L.J. performed chemogenetic and optogenetic experiments. X.S., S.W., and J.W. performed whole-mount immunolabeling. H.X. and H.H. wrote the manuscript with input from H.W. and X.C. All authors validated and approved the final manuscript.

Ethics approval and consent to participate

All animal experiments were approved by the Institutional Animal Care and Use Committee of China Pharmaceutical University and adhered to the principles outlined in the Guide for the Care and Use of Laboratory Animals.

Abbreviations

AUC: area under the curve
CG: celiac ganglion
CGRP: Calcitonin gene-related peptide,
CNS: central nervous system
ChR2: channelrhodopsin-2
ELISA: enzyme-linked immunosorbent assay
EPI: epinephrine
G6PC: glucose-6-phosphatase
HPA: hypothalamic-pituitary-adrenal
LPGi: lateral paragigantocellular nucleus
NE: norepinephrine
6-OHDA: 6-hydroxydopamine
PAS: periodic acid-Schiff
PEPCK: phosphoenolpyruvate carboxykinase
PRV: pseudorabies virus; GS, glycogen synthase
PYGL: glycogen phosphorylase
WGA: wheat germ agglutinin

Funding

Funder	Grant reference number	Author
MOST | National Natural Science Foundation of China (NSFC)	82301436	Hao Xie
MOST | National Natural Science Foundation of China (NSFC)	82371311	Hao Xie
MOST | National Natural Science Foundation of China (NSFC)	81930109	Haiping Hao

MOST | National Natural Science Foundation of China (NSFC)	82321005	Haiping Hao
MOST | National Key Research and Development Program of China (NKPs)	2021YFA1301300	Haiping Hao
MOST | National Key Research and Development Program of China (NKPs)	2023YFA1801900	Hao Xie
JST | Natural Science Foundation of Jiangsu Province (Jiangsu Natural Science Foundation)	BK20221050	Hao Xie
JST | Natural Science Foundation of Jiangsu Province (Jiangsu Natural Science Foundation)	BG2024045	Haiping Hao
111 Plan | Overseas Expertise Introduction Project for Discipline Innovation	G20582017001	Haiping Hao
Jiangsu Specially Appointed Professor Program, and the International Postdoctoral Talent Recruitment Program, the Postgraduate Research & Practice Innovation Program of Jiangsu Province	KYCX25_1076	Hao Xie

Author ORCID iDs

Haiping Hao: https://orcid.org/0000-0003-2522-7546
Hao Xie: https://orcid.org/0009-0009-4778-2912

Additional files

RAW WB DATA

References

1. **Corballis MC** (2014) Left brain, right brain: Facts and fantasies. *PLOS Biology* **12**:e1001767 https://doi.org/10.1371/journal.pbio.1001767 | PubMed
2. **Ocklenburg S,** Guo ZV (2024) Cross-hemispheric communication: Insights on lateralized brain functions. *Neuron* **112**:1222-1234 https://doi.org/10.1016/j.neuron.2024.02.010 | PubMed
3. **Tian Z,** Song J, Zhao X, Zhou Y, Chen X, Le Q, et al. (2024) The interhemispheric amygdala-accumbens circuit encodes negative valence in mice. *Science* **386**:eadp7520 https://doi.org/10.1126/science.adp7520 | PubMed
4. **Concha ML,** Bianco IH, Wilson SW (2012) Encoding asymmetry within neural circuits. *Nat Rev Neurosci* **13**:832-843 https://doi.org/10.1038/nrn3371 | PubMed
5. **Güntürkün O,** Diekamp B, Manns M, Nottelmann F, Prior H, Schwarz A, et al. (2000) Asymmetry pays: Visual lateralization improves discrimination success in pigeons. *Current Biology* **10**:1079-1081 https://doi.org/10.1016/s0960-9822(00)00671-0 | PubMed
6. **Wittling W,** Block A, Genzel S, Schweiger E (1998) Hemisphere asymmetry in parasympathetic control of the heart. *Neuropsychologia* **36**:461-468 https://doi.org/10.1016/s0028-3932(97)00129-2 | PubMed
7. **Gershon MD** (1967) Inhibition of gastrointestinal movement by sympathetic nerve stimulation: The site of action. *The Journal of Physiology* **189**:317-327 https://doi.org/10.1113/jphysiol.1967.sp008170 | PubMed
8. **Cano G,** Card JP, Sved AF (2004) Dual viral transneuronal tracing of central autonomic circuits involved in the innervation of the two kidneys in rat. *Journal of Comparative Neurology* **471**:462-481 https://doi.org/10.1002/cne.20040 | PubMed
9. **Dum RP,** Levinthal DJ, Strick PL (2016) Motor, cognitive, and affective areas of the cerebral cortex influence the adrenal medulla. *Proceedings of the National Academy of Sciences* **113**:9922-9927 https://doi.org/10.1073/pnas.1605044113 | PubMed

10. **Li X,** Zhou Y, Wang F, Wang L (2024) Sex-dimorphic kidney-brain connectivity map of mice. *Neurosci Bull* **40**:1445-1457 https://doi.org/10.1007/s12264-024-01240-z | PubMed
11. **Kirchner A** (2002) Sex differences and lateral asymmetry in heart rate modulation in patients with temporal lobe epilepsy. Journal of Neurology. *Neurosurgery & Psychiatry* **73**:73-75 https://doi.org/10.1136/jnnp.73.1.73 | PubMed
12. **Levinthal DJ,** Strick PL (2020) Multiple areas of the cerebral cortex influence the stomach. *Proceedings of the National Academy of Sciences* **117**:13078-13083 https://doi.org/10.1073/pnas.2002737117 | PubMed
13. **Miller BM,** Oderberg IM, Goessling W (2021) Hepatic nervous system in development, regeneration, and disease. *Hepatology* **74**:3513 https://doi.org/10.1002/hep.32055 | PubMed
14. **Liu K,** Yang L, Wang G, Liu J, Zhao X, Wang Y, et al. (2021) Metabolic stress drives sympathetic neuropathy within the liver. *Cell Metabolism* **33**:666-675. https://doi.org/10.1016/j.cmet.2021.01.012 | PubMed
15. **Mizuno K,** Ueno Y (2017) Autonomic nervous system and the liver. *Hepatology Research* **47**:160-165 https://doi.org/10.1111/hepr.12760 | PubMed
16. **Matsubara Y,** Kiyohara H, Teratani T, Mikami Y, Kanai T (2022) Organ and brain crosstalk: The liver-brain axis in gastrointestinal, liver, and pancreatic diseases. *Neuropharmacology* **205**:108915 https://doi.org/10.1016/j.neuropharm.2021.108915 | PubMed
17. **Tanimizu N,** Ichinohe N, Mitaka T (2018) Intrahepatic bile ducts guide establishment of the intrahepatic nerve network in developing and regenerating mouse liver. *Development* **145**:dev159095 https://doi.org/10.1242/dev.159095 | PubMed
18. **Wang T,** Teng B, Yao DR, Gao W, Oka Y (2025) Organ-specific sympathetic innervation defines visceral functions. *Nature* **637**:895-902 https://doi.org/10.1038/s41586-024-08269-0 | PubMed
19. **Torres H,** Huesing C, Burk DH, Molinas AJR, Neuhuber WL, Berthoud H-R, et al. (2021) Sympathetic innervation of the mouse kidney and liver arising from prevertebral ganglia. *American Journal of Physiology-Regulatory, Integrative and Comparative Physiology* **321**:R328-R337 https://doi.org/10.1152/ajpregu.00079.2021 | PubMed
20. **Wang J,** Sun X, Gong X, Dai W, Hong H, Jiang L, Wang Z, Tang Z, Wu X, Sun P, *et al.* (2025) Galnt2 neurons in the ventromedial hypothalamus counterregulate hypoglycemia via a brain-liver neurocircuit. *Cell Metab* **37**:2264-2279. https://doi.org/10.1016/j.cmet.2025.09.006 | PubMed
21. **Gerendai I,** Tóth IE, Boldogkői Z, Halász B (2009) Recent findings on the organization of central nervous system structures involved in the innervation of endocrine glands and other organs; observations obtained by the transneuronal viral double-labeling technique. *Endocr* **36**:179-188 https://doi.org/10.1007/s12020-009-9189-8 | PubMed
22. **Desmoulins LD,** Molinas AJR, Dugas CM, Williams GL, Kamenetsky S, Davis RK, Derbenev AV, Zsombok A (2025) A subset of neurons in the paraventricular nucleus of the hypothalamus directly project to liver-related premotor neurons in the ventrolateral medulla. *Auton Neurosci* **257**:103222 https://doi.org/10.1016/j.autneu.2024.103222 | PubMed
23. **Stanley S,** Pinto S, Segal J, Pérez CA, Viale A, DeFalco J, Cai X, Heisler LK, Friedman JM (2010) Identification of neuronal subpopulations that project from hypothalamus to both liver and adipose tissue polysynaptically. *Proc Natl Acad Sci U S A* **107**:7024-9 https://doi.org/10.1073/pnas.1002790107 | PubMed
24. **Hwang J,** Lee S, Okada J, Liu L, Pessin JE, Chua SC, Schwartz GJ, Jo YH (2025) Liver-innervating vagal sensory neurons are indispensable for the development of hepatic steatosis and anxiety-like behavior in diet-induced obese mice. *Nat Commun* **16**:991 https://doi.org/10.1038/s41467-025-56328-5 | PubMed
25. **Okumura K,** Grace H, Sogawa H, Yamanaga S (2022) Acute kidney injury and the compensation of kidney function after nephrectomy in living donation. *World Journal of Transplantation* **12**:223-230 https://doi.org/10.5500/wjt.v12.i8.223 | PubMed

26. **Kaufman JM,** DiMeola HJ, Siegel NJ, Lytton B, Kashgarian M, Hayslett JP (1974) Compensatory adaptation of structure and function following progressive renal ablation. *Kidney International* **6**:10-17 https://doi.org/10.1038/ki.1974.72 | PubMed

27. **Dallman M,** Engeland W, Shinsako J (1976) Compensatory adrenal growth: A neurally mediated reflex. *American Journal of Physiology-Legacy Content* **231**:408-414 https://doi.org/10.1152/ajplegacy.1976.231.2.408 | PubMed

28. **Bech J,** Glud AN, Sangill R, Petersen M, Frandsen J, Orlowski D, West MJ, Pedersen M, Sørensen JCH, Dyrby TB, *et al.* (2018) The porcine corticospinal decussation: A combined neuronal tracing and tractography study. *Brain Res Bull* **142**:253-262 https://doi.org/10.1016/j.brainresbull.2018.08.004 | PubMed

29. **Brinkman J,** Kuypers HG (1973) Cerebral control of contralateral and ipsilateral arm, hand and finger movements in the split-brain rhesus monkey. *Brain* **96**:653-74 https://doi.org/10.1093/brain/96.4.653 | PubMed

30. **Larsson M** (2013) The optic chiasm: a turning point in the evolution of eye/hand coordination. *Front Zool* **10**:41 https://doi.org/10.1186/1742-9994-10-41 | PubMed

31. **Bisazza A,** J. Rogers L, Vallortigara G (1998) The origins of cerebral asymmetry: A review of evidence of behavioural and brain lateralization in fishes, reptiles and amphibians. *Neuroscience & Biobehavioral Reviews* **22**:411-426 https://doi.org/10.1016/s0149-7634(97)00050-x | PubMed

32. **Güntürkün O,** Ströckens F, Ocklenburg S (2020) Brain lateralization: A comparative perspective. *Physiological Reviews* **100**:1019-1063 https://doi.org/10.1152/physrev.00006.2019 | PubMed

33. **Zeng W,** Yang F, Shen WL, Zhan C, Zheng P, Hu J (2022) Interactions between central nervous system and peripheral metabolic organs. *Sci China Life Sci* **65**:1929-1958 https://doi.org/10.1007/s11427-021-2103-5 | PubMed

34. **Sun M,** Wan Y, Shi M, Meng Z-X, Zeng W (2023) Neural innervation in adipose tissue, gut, pancreas, and liver. *Life Metabolism* **2**:load022 https://doi.org/10.1093/lifemeta/load022 | PubMed

35. **Abramov VV,** Gontova IA, Kozlov VA (2001) Functional asymmetry of thymus and the immune response in mice. *Neuroimmunomodulation* **9**:218-224 https://doi.org/10.1159/000049029 | PubMed

36. **Tao J,** Campbell JN, Tsai LT, Wu C, Liberles SD, Lowell BB (2021) Highly selective brain-to-gut communication via genetically defined vagus neurons. *Neuron* **109**:2106-2115. https://doi.org/10.1016/j.neuron.2021.05.004 | PubMed

37. **Barron SA,** Rogovski Z, Hemli J (1994) Autonomic consequences of cerebral hemisphere infarction. *Stroke* **25**:113-116 https://doi.org/10.1161/01.str.25.1.113 | PubMed

38. **Qiu L,** Zhang B, Gao Z (2022) Lighting up neural circuits by viral tracing. *Neurosci Bull* **38**:1383-1396 https://doi.org/10.1007/s12264-022-00860-7 | PubMed

39. **Adori C,** Daraio T, Kuiper R, Barde S, Horvathova L, Yoshitake T, et al. (2021) Disorganization and degeneration of liver sympathetic innervations in nonalcoholic fatty liver disease revealed by 3D imaging. *Sci Adv* **7**:eabg5733 https://doi.org/10.1126/sciadv.abg5733 | PubMed

40. **Xie H,** Heier C, Meng X, Bakiri L, Pototschnig I, Tang Z, Schauer S, Baumgartner VJ, Grabner GF, Schabbauer G, *et al.* (2022) An immune-sympathetic neuron communication axis guides adipose tissue browning in cancer-associated cachexia. *Proc Natl Acad Sci U S A* **119**:e2112840119 https://doi.org/10.1073/pnas.2112840119 | PubMed

41. **Edwards AV,** Silver M (1972) Comparison of the hyperglycaemic and glycogenolytic responses to catecholamines with those to stimulation of the hepatic sympathetic innervation in the dog. *The Journal of Physiology* **223**:571-593 https://doi.org/10.1113/jphysiol.1972.sp009863 | PubMed

42. **Garceau D,** Yamaguchi N, Goyer R, Guitard F (1984) Correlation between endogenous noradrenaline and glucose released from the liver upon hepatic sympathetic nerve stimulation in anesthetized dogs. *Can J Physiol Pharmacol* **62**:1086-1091 https://doi.org/10.1139/y84-181 | PubMed

43. **Järhult J,** Andersson P -O, Holst J, Moghimzadeh E, Nobin A (1980) On the sympathetic innervation to the cat's liver and its role for hepatic glucose release. *Acta Physiologica Scandinavica* **110**:5-11 https://doi.org/10.1111/j.1748-1716.1980.tb06623.x | PubMed

44. **Gardemann A,** Strulik H, Jungermann K (1987) Nervous control of glycogenolysis and blood flow in arterially and portally perfused liver. *Am J Physiol* **253**:E238-45 https://doi.org/10.1152/ajpendo.1987.253.3.e238 | PubMed

45. **Hartmann H,** Beckh K, Jungermann K (1982) Direct control of glycogen metabolism in the perfused rat liver by the sympathetic innervation. *Eur J Biochem* **123**:521-6 https://doi.org/10.1111/j.1432-1033.1982.tb06562.x | PubMed

46. **Vanderauwera J,** Hellemans E, Verhaert N (2020) Research Insights on Neural Effects of Auditory Deprivation and Restoration in Unilateral Hearing Loss: A Systematic Review. *J Clin Med* **9**:812 https://doi.org/10.3390/jcm9030812 | PubMed

47. **Alzaher M,** Strelnikov K, Marx M, Barone P (2023) Brain plasticity and auditory spatial adaptation in patients with unilateral hearing loss. *Cereb Cortex* **33**:7221-7236 https://doi.org/10.1093/cercor/bhad033 | PubMed

48. **Zhao S,** Todorov MI, Cai R, Maskari RA, Steinke H, Kemter E, et al. (2020) Cellular and molecular probing of intact human organs. *Cell* **180**:796-812. https://doi.org/10.1016/j.cell.2020.01.030 | PubMed

49. **Cai R,** Pan C, Ghasemigharagoz A, Todorov MI, Förstera B, Zhao S, et al. (2019) Panoptic imaging of transparent mice reveals whole-body neuronal projections and skull-meninges connections. *Nature neuroscience* **22**:317-327 https://doi.org/10.1038/s41593-018-0301-3 | PubMed

Peer reviews

Reviewer #2 (Public review):

Summary:

The manuscript by Wang and colleagues aims to determine whether hepatic glucose metabolism is differentially regulated by the left and right sides of the LPGi and to reveal decussation of hepatic sympathetic nerves.

The authors used tissue clearing to identify sympathetic fibers in the liver lobes, then injected PRV into the hepatic lobes. Five days post-injection, PRV-labeled neurons in the LPGi, which were identified. The results indicated contralateral dominance of premotor neurons and partial innervation of more than one lobe. Then the authors activated each side of the LPGi, resulting in a greater increase in blood glucose levels after right-sided activation than after left-sided activation, and in changes in protein expression in the liver lobes. These data suggested lobe-specific modulation of HGP. Chemical denervation of a particular lobe did not affect glucose levels due to compensation by the other lobes. In addition, nerve bundles decussate in the hepatic portal region.

Strengths:

The manuscript is timely and relevant. It is important to understand the sympathetic regulation of the liver and the contribution of each lobe to hepatic glucose production. The authors use state-of-the-art methodology.

Weaknesses:

(1) Image clarity was improved in some cases, but not in others. For example, Figure 3I, showing c-Fos expression, is not convincing due to the image quality and lack of orientation.

(2) The methods section states that 8-weeks-old male mice were used in the experiments without specifying the experiments (e.g., brain injection with AAVs or PRV organ inoculation).

The authors should include these details.

(3) The authors should use the exact location of pre- and postganglionic neurons as they often refer to neurons in the sympathetic chain. Their findings should be compared with the existing literature on the location of preganglionic cells.

(4) Figure legends should be revised and matched with the text.

https://doi.org/10.7554/eLife.109599.2.sa2

Reviewer #4 (Public review):

Summary of General Strengths & Weaknesses:

The studies here are highly informative for anatomical tracing and sympathetic nerve function in the liver in relation to glucose levels, but because they are conducted in a single species, it is challenging to translate them to humans or determine whether these neural circuits are evolutionarily conserved. Dual-labeling anatomical studies are elegant, and the addition of chemogenetic and optogenetic studies provides mechanistically informative. Denervation studies lack proper controls, and sensory innervation in the liver is overlooked.

Specific Weaknesses - Major:

(1) The species name should be included in the title.

(2) Tyrosine hydroxylase was used to mark sympathetic fibers in the liver, but this marker also labels a portion of sensory fibers that need to be ruled out in whole-mount imaging data.

(3) Chemogenetic and optogenetic data demonstrating hyperglycemia should be described in the context of prior work demonstrating liver nerve involvement in these processes. There is only a brief mention in the Discussion currently, but comparing methods and observations would be helpful.

(4) Sympathetic denervation with 6-OHDA can drive compensatory increases in tissue sensory innervation, and this should be measured in the liver denervation studies to implicate potential crosstalk, especially given the increase in LPGi cFOS that may be due to afferent nerve activity. Compensatory sympathetic drive may not be the only culprit, though that is clearly assumed. The sensory or parasympathetic/vagal innervation of the liver is altogether ignored in this paper and could be better described in general.

Comments on the revised version.

Across all reviewer comments, the revised resubmission has adequately addressed all concerns.

https://doi.org/10.7554/eLife.109599.2.sa1

Author response:

The following is the authors' response to the original reviews.

> ***Public Reviews:***
>
> ***Reviewer #1 (Public review):***
>
> *Summary:*

> *This manuscript by Wang et al. reports the potential involvement of an asymmetric neurocircuit in the sympathetic control of liver glucose metabolism.*
>
> *Strengths:*
>
> *The concept that the contralateral brain-liver neurocircuit preferentially regulates each liver lobe may be interesting.*
>
> *Weaknesses:*
>
> *However, the experimental evidence presented did not support the study's central conclusion.*

We thank the reviewer for recognizing the conceptual novelty of our work and for constructive comments aimed at enhancing its rigor and clarity. In response, we carried out targeted experiments to address the points raised, including: (i) further characterization of LPGi projections to vagal and sympathetic circuits; (ii) evaluation of potential pancreatic involvement; and (iii) validation of the specificity of chemogenetic activation within the proposed circuit. All new experiments, figures, and text have been incorporated, and corresponding revisions are highlighted for ease of review.

> *(1) Pseudorabies virus (PRV) tracing experiment:*
>
> *The liver not only possesses sympathetic innervations but also vagal sensory innervations. The experimental setup failed to distinguish whether the PRV-labeling of LPGi (Lateral Paragigantocellular Nucleus) is derived from sympathetic or vagal sensory inputs to the liver.*

Thank you for raising this important point. We fully agree that the liver receives both sympathetic and vagal sensory innervation, and we acknowledge that PRV-based tracing alone does not definitively distinguish between these two pathways. This represented a limitation of the original experimental design.

Based on established anatomical literature as well as our experimental observations, vagal sensory neuron cell bodies reside in the nodose ganglion (NG), and their central projections terminate predominantly in the nucleus of the solitary tract (NTS) (Nature. 2023;623(7986):387-396; Curr Biol. 2020;30(20):3986-3998.e5.), which is located in the dorsomedial medulla. In contrast, the LPGi, together with other sympathetic-related nuclei, is predominantly distributed in the ventral medulla (Cell Metab. 2025;37(11):2264-2279.e10; Nat Commun. 2022;13(1):5079).

To determine whether the LPGi contains neurons that modulate the liver via vagal sensory pathways, we performed two complementary experiments.

First, we conducted CGRP immunohistochemistry on brainstem sections, using the NTS, a well-established visceral sensory centre, as a positive control. While abundant CGRP-positive cell bodies were detected in the NTS as expected, few to no CGRP-positive cell bodies were observed in the LPGi (Figure S1G). These results strongly support that the LPGi neurons labeled in our PRV tracing predominantly belong to sympathetic efferent circuits rather than vagal sensory pathways.

Second, to examine whether LPGi neurons send axonal projections to sensory ganglia, we injected hSyn-Cre combined with DIO-Axon-EGFP into the LPGi and examined both the dorsal root ganglia (DRG) and nodose ganglia (NG). No Axon-EGFP-positive signals were detected in either ganglion (Figures S1H-S1J), indicating that LPGi neurons do not directly innervate sensory ganglia. In other words, PRV cannot retrogradely trace to the LPGi via the NG or DRG.

These additions have been incorporated into the revised manuscript, with the Result 1 clearly documenting that these findings confirm that the LPGi specifically regulates sympathetic, rather than vagal sensory, inputs to the liver.

> *(2) Impact on pancreas:*
>
> *The celiac ganglia not only provide sympathetic innervations to the liver but also to the pancreas, the central endocrine organ for glucose metabolism. The chemogenetic manipulation of LPGi failed to consider a direct impact on the secretion of insulin and glucagon from the pancreas.*

Thank you for this important comment. We agree that the celiac ganglia (CG) provide sympathetic innervation not only to the liver but also to the pancreas, which plays a central role in glucose homeostasis through the secretion of both insulin and glucagon. Therefore, the potential pancreatic implications associated with LPGi chemogenetic manipulation are worth careful consideration.

To address this concern, we measured circulating glucagon and insulin levels following chemogenetic manipulation of the $LPGi^{GAD1}$ neurons. We found that neither glucagon nor insulin levels changed significantly under our experimental conditions, which indicated that the hyperglycemic effect induced by LPGi activation is unlikely to be mediated by changes in pancreatic hormone secretion (Figure S2G).

These additions have been incorporated into the revised manuscript, with the Result 2 clearly documenting that these findings confirm that the hyperglycemic effect induced by LPGi activation is unlikely to be mediated indirectly via altered pancreatic endocrine output.

> *(3) Neuroanatomy of the brain-liver neurocircuit:*
>
> *The current study and its conclusion are based on a speculative brain-liver sympathetic circuit without the necessary anatomical information downstream of LPGi.*

Thank you for raising this important point. A clear anatomical definition of the downstream pathways linking the brain to the liver was essential for interpreting the proposed brain-liver sympathetic circuit.

The present study (Figure 4A) provides direct anatomical evidence supporting the organization of the brain–liver sympathetic neurocircuit. These observations are consistent with our recent detailed characterization of the brain-liver sympathetic circuit published in Cell Metabolism (Cell Metab. 2025;37(11):2264–2279). In that study, we showed that LPGi GABAergic neurons inhibit GABAergic neurons in the caudal ventrolateral medulla (CVLM). Disinhibition of CVLM reduced GABAergic suppression of rostral ventrolateral medulla (RVLM) neurons, which are key excitatory drivers of sympathetic tone. RVLM neurons project to sympathetic preganglionic neurons in the sympathetic chain (Syc). These neurons synapse with postganglionic sympathetic neurons in ganglia such as the celiac-superior mesenteric ganglion (CG-SMG). Postganglionic sympathetic fibers then innervate the liver, releasing norepinephrine (NE) to activate hepatic β_2-adrenergic receptors and stimulate hepatic glucose production (HGP).

Together, these data establish a coherent anatomical basis for the proposed brain-liver sympathetic pathway and clarify the downstream organization relevant to the functional experiments presented in figure 4A and Author response image 1..

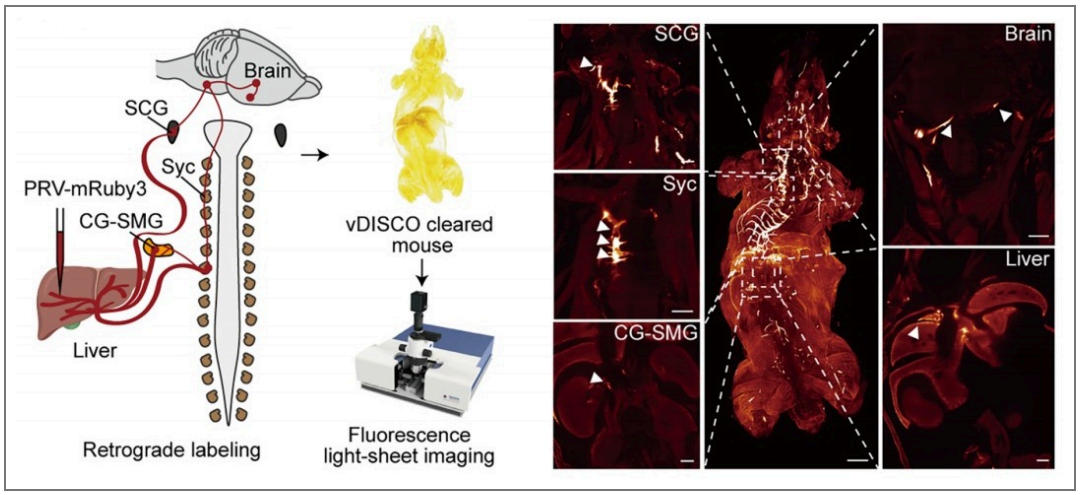

Author response image 1. Tracing scheme (Left) and whole-mount imaging (Right) of PRV-labeled brain-liver neurocircuit. Scale bars, 3,000 (whole mount) or 1,000 (optical sections) μm.

> *(4) Local manipulation of the celiac ganglia:*
>
> *The left and right ganglia of mice are not separate from each other but rather anatomically connected. The claim that the local injection of AAV in the left or right ganglion without affecting the other side is against this basic anatomical feature.*

Thank you for raising this important anatomical point. We fully acknowledge that the left and right CG in mice are interconnected, and that unilateral viral injection could theoretically affect the contralateral side. The CG-SMG complex serves as a major sympathetic hub that regulates visceral organ functions. Recent transcriptomic, anatomical, and functional studies have revealed that the CG-SMG is not a homogeneous structure but is composed of molecularly and functionally distinct neuronal populations. These populations exhibit specialized projection patterns and regulate different aspects of gastrointestinal physiology, supporting a model of modular sympathetic control. (Nature. 2025 Jan;637(8047):895-902). Therefore, we were aware of this phenomenon during the initial stages of these experiments.

To minimize unintended spread to the contralateral CG, we took two complementary approaches.

First, we optimized the injection strategy by using an extremely small injection volume (100 nL per site), with a very slow infusion rate (50 nL/min), and fine glass micropipettes. With these refinements, contralateral viral spread was rarely observed.

Second, and importantly, all animals included in the final analyses were subjected to post hoc anatomical verification. After completion of the experiments, CGs were collected, sectioned, and examined for viral expression. As shown in Supplementary Figure 5F, only mice in which viral expression was strictly confined to the targeted CG, with no detectable infection in the contralateral ganglion, were included in the presented data.

Together, these measures ensure that our local manipulation of the intended CG produced the reported effects. We have revised the Methods section to more explicitly detail these technical precautions, and the legend for Figure S5F clearly states its role in validating injection specificity.

> ***Reviewer #2 (Public review):***
>
> *Summary:*

> *The manuscript by Wang and colleagues aims to determine whether the left and right LPGi differentially regulate hepatic glucose metabolism and to reveal decussation of hepatic sympathetic nerves.*
>
> *The authors used tissue clearing to identify sympathetic fibers in the liver lobes, then injected PRV into the hepatic lobes. Five days post-injection, PRV-labeled neurons in the LPGi were identified. The results indicated contralateral dominance of premotor neurons and partial innervation of more than one lobe. Then the authors activated each side of the LPGi, resulting in a greater increase in blood glucose levels after right-sided activation than after left-sided activation, as well as changes in protein expression in the liver lobes. These data suggested modulation of HGP (hepatic glucose production) in a lobe-specific manner. Chemical denervation of a particular lobe did not affect glucose levels due to compensation by the other lobes. In addition, nerve bundles decussate in the hepatic portal region.*

We thank the reviewer for the thorough and constructive evaluation of our manuscript. In direct response, we undertook comprehensive revisions to enhance the rigor and clarity of the study, including: (i) correcting ambiguous or misleading terminology about anatomical resolution and sympathetic circuit organization; (ii) expanding the Methods section with complete experimental details, improved image presentation, and explicit justification of our viral and genetic approaches; and (iii) strengthening data interpretation by addressing issues related to sparse PRV labeling, projection heterogeneity, and the functional implications of double-labeled neurons.

> *Strengths:*
>
> *The manuscript is timely and relevant. It is important to understand the sympathetic regulation of the liver and the contribution of each lobe to hepatic glucose production. The authors use state-of-the-art methodology.*
>
> *Weaknesses:*
>
> *(1) The wording/terminology used in the manuscript is misleading, and it is not used in the proper context. For instance, the goal of the study is "to investigate whether cerebral hemispheres differentially regulate hepatic glucose metabolism..." (see abstract); however, the authors focus on the brainstem (a single structure without hemispheres). Similarly, symmetric is not the best word for the projections.*

We thank the reviewer for raising these critical points regarding terminology and conceptual framing. We acknowledge that certain phrases in our original manuscript may have been overly broad or ambiguous, particularly in describing the scope of sympathetic heterogeneity and the specificity of neural projections. Due to practical constraints and the scope of our study, our investigation focused on the brainstem, which represents the final common pathway for these lateralized commands. We acknowledge that terms referring to the cerebral hemispheres do not accurately describe our study. We have revised the manuscript to ensure accurate and consistent terminology.

Below are specific examples:

Original 1: This study aims to investigate whether cerebral hemispheres differentially regulate hepatic glucose metabolism and localize the site of sympathetic crossover to the liver.

Revised 1: “This study aimed to determine whether the central nervous system exerts lateralized control over hepatic glucose metabolism and to localize the site of peripheral sympathetic crossover to the liver.”

Original 2: These findings demonstrate that the brain exerts lobe-specific, lateralized control of hepatic glucose metabolism via symmetric brain-liver sympathetic pathways.

Revised 2: “These findings demonstrate that the brainstem can exert lobe-specific, lateralized control of hepatic glucose metabolism via bilaterally projecting brain–liver sympathetic pathways.”

Original 3: The cerebral hemispheres exhibit pronounced functional asymmetry, [1,2] a phenomenon traditionally associated with cognitive and motor processes such as language, voluntary movement, and spatial navigation.[3,4]

Revised 3: “Pronounced functional lateralization within the central nervous system (CNS) is a well-documented phenomenon, [1,2] traditionally associated with cognitive and motor processes such as language, voluntary movement, and spatial navigation [3,4].

> *(2) Sparse labeling of liver-related neurons was shown in the LPGi (Figure 1). It would be ideal to have lower magnification images to show the area. Higher quality images would be necessary, as it is difficult to identify brainstem areas. The low number of labeled neurons in the LPGi after five days of inoculation is surprising. Previous findings showed extensive labeling in the ventral brainstem at four days post-inoculation (Desmoulins et al., 2025). Unfortunately, it is not possible to compare the injection paradigm/methods because the PRV inoculation is missing from the methods section. If the PRV is different from the previously published viral tracers, time-dependent studies to determine the order of neurons and the time course of infection would be necessary.*

We sincerely thank the reviewer for these detailed and constructive comments regarding the PRV tracing experiments. We fully agree that careful presentation and interpretation of the anatomical data are essential for ensuring rigor and transparency. We address each point in detail below.

(1) Image magnification and anatomical context of LPGi labeling

We agree that the original images did not sufficiently convey the broader anatomical context of the LPGi. Due to fluorescence quenching in previous sections, we repeated the PRV retrograde tracing experiment and performed statistical analysis. In the revised manuscript, we replaced the original panels in Figure 1 and Figure S1 with new images that include lower-magnification overviews of the brainstem, alongside higher-magnification views of the LPGi (Figure 1). These images clearly delineate the LPGi with respect to established anatomical landmarks and atlas boundaries. Image contrast and resolution were optimized to allow unambiguous identification of PRV-labeled neurons and surrounding structures.

(2) Sparse LPGi labeling at 5 days post-injection and methodological details

We apologize for the omission of the detailed PRV injection protocol in the original Methods section. We deliberately used small-volume, local injections (1 μL per liver lobe) to minimize viral spread and to restrict labeling to circuits specifically connected to the targeted hepatic region. This sparse labeling was consistent with the use of small, spatially restricted injections designed to minimize off-target spread and preferentially label higher-order upstream neurons. This information has now been added, including the PRV strain, viral titer, injection volume, precise injection coordinates, and surgical procedures. All new figures, legends, and Method details have been incorporated, with changes clearly highlighted for ease of review.

These additions have been incorporated into the revised manuscript, in Figure 1B-D, Figure S1C-F. Furthermore, we also added details of the Methods.

> *(3) Not all LPGi cells are liver-related. Was the entire LPGi population stimulated, or was it done in a cell-type-specific manner? What was the strain, sex, and age of the mice? What was the rationale for using the particular viral constructs?*

We thank the reviewer for this insightful and important question. We agree that not all neurons within the LPGi are liver-related, and we apologize that our rationale was not clearly articulated in the original manuscript.

(1) Our decision to target GABAergic neurons in the LPGi using GAD1-Cre mice was based on prior experimental evidence rather than an assumption about the entire LPGi population. In our previous study (Cell Metab. 2025;37(11):2264-2279.e10), we performed single-cell RNA sequencing on retrogradely labeled LPGi neurons following liver tracing. These analyses revealed that the majority of liver-projecting LPGi neurons are GABAergic in nature. Based on these findings, we chose to selectively manipulate GABAergic neurons in the LPGi rather than the entire LPGi neuronal population, to achieve greater cellular specificity and to minimize potential confounding effects arising from heterogeneous neuron types within this region. We regret that this rationale was not clearly described in the original submission and have now revised the manuscript to explicitly state this reasoning (Results section 2, paragraph 2: “Prior single-nucleus RNA sequencing and immunofluorescence analyses demonstrated that liver-projecting LPGi neurons are predominantly GABAergic.”).

(2) In addition, we apologize for the omission of mouse strain, sex, and age information in the Methods section. These details have been fully added.

(3) We selected AAV-based viral vectors, specifically the AAV9 serotype, due to their well-established efficiency in transducing neurons in the brainstem, relatively low toxicity, and widespread use in circuit-level chemogenetic and optogenetic studies. When combined with Cre-dependent viral constructs in GAD1-Cre mice, this approach enabled selective and reliable manipulation of LPGi GABAergic neurons.

> *(4) The authors should consider the effect of stimulation of double-labeled neurons (innervating more than one lobe) and potential confounding effects regarding other physiological functions.*

We thank the reviewer for raising this important point. We agree that neurons innervating more than one liver lobe could, in principle, introduce potential confounding effects and may reflect higher-order integrative autonomic neurons.

This consideration is consistent with a key finding of the cited study: the CG-SMG contains molecularly distinct sympathetic neuron populations (e.g., $RXFP1^+$ vs. $SHOX2^+$) that exhibit complementary organ projections and separate, non-overlapping functions. Specifically, $RXFP1^+$ neurons innervate secretory organs (pancreas, bile duct) to regulate secretion, while $SHOX2^+$ neurons innervate the gastrointestinal tract to control motility. This functional segregation supports the concept of specialized autonomic modules rather than a uniform, “fight-or-flight” response, reinforcing the need for careful interpretation of circuit-specific manipulations. (Nature. 2025;637(8047):895-902; Neuron. 2026;114(3):463-478.e7).

In our PRV tracing experiments, the proportion of double-labeled neurons was relatively small, suggesting that the majority of labeled LPGi neurons preferentially associate with individual hepatic lobes. Nevertheless, we recognize that activation of this minority population could contribute to broader physiological effects beyond strictly lobe-specific regulation. We have therefore added a paragraph in the second paragraph of the Discussion (Paragraph 2: “A small subset of LPGi neurons was double-labeled after bilateral PRV injections, suggesting a fraction of these neurons projects bilaterally to both sides of the liver. Such neurons may support interlobar coordination.”).

> *(5) The authors state that "central projections directly descend along the sympathetic chain to the celiac-superior mesenteric ganglia". What they mean is unclear. Do the authors refer to pre-ganglionic neurons or premotor neurons? How does it fit with the previous literature?*

We thank the reviewer for pointing out this imprecise wording. We agree that the original phrasing was anatomically inaccurate and potentially confusing. The pathways we intended to describe involve brainstem premotor neurons that project to sympathetic preganglionic neurons in the spinal cord. These preganglionic neurons then innervate neurons in the CG-SMG, which in turn provide postganglionic input to the liver.

We have revised the manuscript to clearly distinguish premotor from preganglionic neurons (Results section 4, paragraph 1: “Using whole-mount clearing, we visualized the brain–liver sympathetic circuit and found that preganglionic neurons in the spinal cord send descending fibers through the sympathetic chain (SyC) to innervate postganglionic neurons in the CG-SMG (Figure 4A). Further whole-mount TH immunostaining showed that TH-positive sympathetic cell bodies within the CG-SMG project to the liver along the hepatic vasculature (Figure 4B and Figure S5F). These observations suggest that the nerve bundles likely decussate at the porta hepatis before entering the individual hepatic lobes.”).

> *(6) How was the chemical denervation completed for the individual lobes?*

We thank the reviewer for raising this important methodological concern. We agree that potential diffusion of 6-OHDA is a critical issue when performing lobe-specific chemical denervation, and we apologize that our original description did not sufficiently clarify how this was controlled.

In the revised Methods section, we provided a detailed description of the denervation procedure, including the injection volume and concentration of 6-OHDA, as well as the physical separation and isolation of individual hepatic lobes during application to minimize diffusion to adjacent tissue.

To directly assess the specificity of the chemical denervation, we included immunofluorescence and Western blot analyses demonstrating a selective reduction of sympathetic markers in the targeted lobe (Figure 3C), with minimal effects on non-targeted lobes. These results support the effectiveness and relative spatial confinement of the 6-OHDA treatment under our experimental conditions.

We thank the reviewer for highlighting this point, which has helped us improve both the clarity and rigor of the manuscript.

> *(7) The Western Blot images look like they are from different blots, but there are no details provided regarding protein amount (loading) or housekeeping. What was the reason to switch beta-actin and alpha-tubulin? In Figures 3F -G, the GS expression is not a good representative image. Were chemiluminescence or fluorescence antibodies used? Were the membranes reused?*

We thank the reviewer for this careful and detailed evaluation of the Western blot data. We apologize that insufficient methodological detail was provided in the original submission.

(1) We would like to clarify that the protein bands shown within each panel were derived from the same membrane. To improve transparency, we provided full, uncropped images of the corresponding membranes in the supplementary materials. In addition, detailed information regarding protein loading amounts, gel conditions, and housekeeping controls has also been added to the Methods section.

(2) The use of different loading controls (β-actin or α-tubulin) reflects a technical consideration rather than an experimental inconsistency. In our experiments, the molecular weight of the TH (62kDa) was too close to that of α-tubulin (55kDa), and β-actin (42kDa) was therefore used to avoid band overlap and to ensure accurate quantification.

(3) Regarding the GS signal shown in Figures 3F–G, we agree that the original representative image was suboptimal. This appears to be related to antibody performance rather than sample quality. To address this, we repeated the Western blot from Figures 3F–G using a newly validated antibody. The original tissue samples had been aliquoted and stored at −80 °C, allowing reliable re-analysis.

(4) All Western blot experiments were detected using chemiluminescence, and membrane stripping and reprobing procedures are now explicitly described in the Methods section.

We thank the reviewer for highlighting these issues, which significantly improve the rigor and clarity of our data presentation. All new figures and legends have been incorporated, with changes clearly highlighted for ease of review.

> *(8) Key references using PRV for liver innervation studies are missing (Stanley et al, 2010 [PMID: 20351287]; Torres et al., 2021 [PMID: 34231420]; Desmoulins et al., 2025 [PMID: 39647176]).*

We thank the reviewer for pointing out these important and highly relevant references that were inadvertently omitted in our initial submission. The studies by Stanley et al. (Proc Natl Acad Sci U S A, 2010), Torres et al. (Am J Physiol Regul Integr Comp Physiol, 2021), and Desmoulins et al. (Auton Neurosci, 2025) represent key PRV-based retrograde tracing work that has mapped central neural circuits innervating the liver and thus provide essential context for our anatomical analyses.

We agree that the inclusion of these studies is necessary to properly situate our findings within the existing literature. Accordingly, we incorporated citations to these references in the revised manuscript and discussed their relationship to our results.

> ***Reviewer #3 (Public review):***
>
> *Summary:*
>
> *This study found a lobe-specific, lateralized control of hepatic glucose metabolism by the brain and provides anatomical evidence for sympathetic crossover at the porta hepatis. The findings are particularly insightful to the researchers in the field of liver metabolism, regeneration, and tumors.*
>
> *Strengths:*
>
> *Increasing evidence suggests spatial heterogeneity of the liver across many aspects of metabolism and regenerative capacity. The current study has provided interesting findings: neuronal innervation of the liver also shows anatomical differences across lobes. The findings could be particularly useful for understanding liver pathophysiology and treatment, such as metabolic interventions or transplantation.*
>
> *Weaknesses:*
>
> *Inclusion of detailed method and Discussion:*

We sincerely thank the reviewer for the positive and constructive feedback, which significantly enhances both the methodological rigor and the broader biological interpretation of our study. In direct response, we revised the Discussion to elaborate on the potential physiological advantages of a lateralized and lobe-specific pattern of liver

innervation. Furthermore, we expanded the Methods section to include a comprehensive description of the quantitative analysis applied to PRV-labeled neurons. Together, these revisions strengthened the manuscript's clarity, depth, and relevance to researchers in hepatic metabolism, regeneration, and disease.

> *(1) The quantitative results of PRV-labeled neurons are presented, and please include the specific quantitative methods.*

We thank the reviewer for this helpful suggestion. We have added a detailed description of the quantitative methods used to analyze PRV-labeled neurons in the revised Methods section. We have now provided detailed information in the Methods section, including the criteria used for cell counting, the anatomical boundaries of the brain regions analyzed, the delineation of regions of interest, and the normalization procedures applied to derive the reported neuron counts. These additions have been incorporated into the revised Methods, with all changes clearly indicated for ease of review.

> *(2) The Discussion can be expanded to include potential biological advantages of this complex lateralized innervation pattern.*

We appreciated the reviewer's suggestion. We have expanded the Discussion to include a paragraph addressing the potential biological significance of lateralized liver innervation. We highlight that this asymmetric organization could allow for more precise, lobe-specific regulation of hepatic metabolism, enable integration of distinct physiological signals, and potentially provide robustness against perturbations. The additional discussion content has been highlighted in the revised version as indicated (Discussion section, paragraph 3: "Bilateral LPGi activation produced additive effects, indicating that both sides of the brainstem can cooperatively regulate hepatic metabolism in a spatially segregated manner. This pattern suggests that hepatic glucose output can be modulated in a lobe-specific, rather than uniform whole-organ, manner.").

> ***Reviewer #4 (Public review):***
>
> *Summary:*
>
> *The studies here are highly informative in terms of anatomical tracing and sympathetic nerve function in the liver related to glucose levels, but given that they are performed in a single species, it is challenging to translated them to humans, or to determine whether these neural circuits are evolutionarily conserved. Dual-labeling anatomical studies are elegant, and the addition of chemogenetic and optogenetic studies is mechanistically informative. Denervation studies lack appropriate controls, and the role of sensory innervation in the liver is overlooked.*

We sincerely appreciate the reviewer's thoughtful evaluation and fully agree that findings derived from a single-species model must be interpreted with caution in relation to human physiology. In direct response, we revised the manuscript to explicitly clarify that all experimental data were obtained in mice and to provide a discussion of the limitations regarding direct extrapolation to humans. Concurrently, we expanded the Discussion section by integrating our findings with recent human and translational studies, including a multicenter clinical trial demonstrating that catheter-based endovascular denervation of the celiac and hepatic arteries significantly improved glycemic control in patients with poorly controlled type 2 diabetes, without major adverse events (Signal Transduct Target Ther. 2025;10(1):371). While our current work focuses on defining the anatomical organization and functional asymmetry of this circuit in mice, the clinical findings suggest that the core principles, sympathetic control of hepatic glucose metabolism via CG-liver pathways, may be conserved and of translational relevance. Additionally, we clarified the interpretation of TH labeling and expanded the discussion of hepatic sensory and parasympathetic innervation,

acknowledging their important roles in liver-brain communication and identifying them as key directions for future research. Collectively, these revisions provide a more balanced, clinically informed, and rigorous framework for interpreting our findings.

> *Specific Weaknesses - Major:*
>
> *(1) The species name should be included in the title.*

We thank the reviewer for this suggestion. We agree that the species should be clearly indicated. The findings presented in this study were obtained in mice using tissue clearing and whole-organ imaging approaches. Due to technical limitations, these observations are currently restricted to the mouse strain. We have updated the title (Symmetric brain-liver circuits mediate lateralized regulation of hepatic glucose output in mice) and clarified the species used throughout the manuscript.

> *(2) Tyrosine hydroxylase was used to mark sympathetic fibers in the liver, but this marker also hits a portion of sensory fibers that need to be ruled out in whole-mount imaging data*

We thank the reviewer for pointing this out. We acknowledge that TH labels not only sympathetic fibers but also a subset of sensory fibers. We have added a limitation of this point in the revised manuscript. In addition, using SyGlass (2.4.0) three-dimensional reconstruction, we observed TH-positive nerve fibers originating from the CG-SMG extending along the porta hepatis and penetrating into the liver parenchyma. Given that the CG-SMG is a well-established sympathetic ganglion innervating visceral organs (Nature. 2025 Jan;637(8047):895-902.), these nerve fibers can be definitively identified as sympathetic. In parallel, we collected DRG from spinal segments T1-6 and T7-12 five days after intrahepatic PRV injection. While T7-12 DRG are known to contain sensory neurons innervating the liver, only a sparse number of PRV-positive neurons were detected in these segments (Anat Rec A Discov Mol Cell Evol Biol. 2004 Sep;280(1):827-35. Auton Neurosci. 2024 Jun;253:103174). The additional figure and discussion content have been highlighted in the revised version as indicated (Discussion section, paragraph 6: “Third, although whole-mount TH immunostaining with three-dimensional reconstruction revealed sympathetic nerve bundles projecting from the CG to the liver, TH is not entirely specific and can also label a subset of sensory neurons. More selective approaches, such as genetic targeting of sympathetic lineages, will be important for further validation.”).

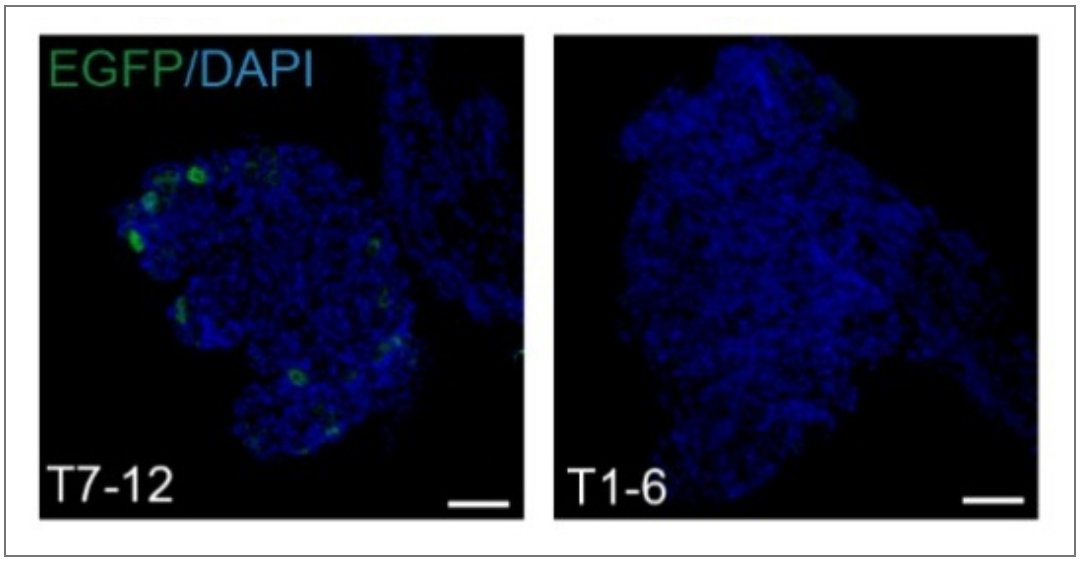

Author response image 2. Representative immunofluorescence images of PRV-labeled neurons (EGFP) in DRG from the spinal segments T1-6 (bottom) and T7-12 (top) following PRV injections into the liver lobes. Scale bars, 200μm

> *(3) Chemogenetic and optogenetic data demonstrating hyperglycemia should be described in the context of prior work demonstrating liver nerve involvement in these processes. There is only a brief mention in the Discussion currently, but comparing methods and observations would be helpful.*

We thank the reviewer for this suggestion. Previous studies largely relied on electrical stimulation to modulate liver innervation, which provides relatively coarse control of neural activity (Eur J Biochem. 1992;207(2):399-411). By contrast, our use of chemogenetic and optogenetic approaches allows selective, cell-type-specific manipulation of LPGi neurons. We revised the Discussion to place our functional data in the context of prior work, highlighting how these more precise approaches improve understanding of the contribution of liver-innervating neurons to hyperglycemia. The newly added discussion has been clearly labeled in the response to facilitate your review (Discussion section, paragraph 3: “This spatial organization is likely obscured by conventional electrical stimulation, which indiscriminately activates heterogeneous sympathetic fibers. By contrast, chemogenetic and optogenetic approaches permit selective, cell type-specific manipulation of LPGi neurons, thereby revealing the contralateral and lobe-specific architecture of brain-liver sympathetic control”).

> *(4) Sympathetic denervation with 6-OHDA can drive compensatory increases to tissue sensory innervation, and this should be measured in the liver denervation studies to implicate potential crosstalk, especially given the increase in LPGi cFOS that may be due to afferent nerve activity. Compensatory sympathetic drive may not be the only culprit, though it is clearly assumed to be. The sensory or parasympathetic/vagal innervation of the liver is altogether ignored in this paper and could be better described in general.*

We thank the reviewer for this insightful and important comment, which highlights a potential alternative interpretation of our findings. We agree that chemical sympathetic denervation with 6-OHDA may induce compensatory changes in non-sympathetic inputs, including sensory and parasympathetic (vagal) innervation of the liver.

Conceptually, we agree with the reviewer’s perspective that the central nervous system operates as a highly integrated homeostatic regulatory system, continuously receiving and integrating a broad range of afferent signals. These inputs include, as noted by the reviewer, hepatic sensory and vagal afferents (Science. 2024;386(6722):673-677), as well as centrally

derived interoceptive signals such as brain glucose, temperature sensing, even the pulsation of cerebral vascular system (Cell Metab. 2025;37(11):2264-2279.e10.; Cell Metab. 2022;34(6):888-901.e5; Science. 2024;383(6682):eadk8511). The CNS integrates these diverse signals and generates coordinated efferent outputs to maintain systemic homeostasis.

From this viewpoint, the changes in c-FOS activity that we observe in the LPGi likely represent only a limited snapshot of this broader integrative process, rather than evidence of a single dominant pathway. We acknowledge that compensatory sensory or parasympathetic mechanisms, in addition to altered sympathetic drive, contributed to the observed LPGi activation following hepatic sympathetic denervation.

We further acknowledge that, due to limitations in scope and experimental focus, we did not directly assess sensory or parasympathetic innervation of the liver in the present study. As appropriately pointed out by the reviewer, a more comprehensive characterization of hepatic neural inputs would provide a more complete picture of the underlying neurocircuitry. To address this, we expanded the Discussion and explicitly noted this limitation, including a more balanced discussion of potential crosstalk among sympathetic, sensory, and parasympathetic pathways and how these may collectively influence LPGi activity. For your convenience, the newly added discussion text has been distinctly marked in the manuscript (Discussion section, paragraph 4: “Although enhanced sympathetic output appears to mediate much of this compensation, our findings suggest that the underlying regulation extends beyond a purely descending pathway. In particular, c-FOS activation in the contralateral LPGi after unilateral 6-OHDA-mediated denervation suggests that the loss of peripheral input may be sensed through an ascending neural pathway, centrally integrated, and translated into compensatory sympathetic output to the intact hepatic lobes. These results therefore support a model in which hepatic glucose production is regulated by an integrated afferent-central-efferent loop, with our current analyses primarily resolving its efferent component.”).

> ***Recommendations for the authors:***
>
> ***Reviewer #2 (Recommendations for the authors):***
>
> *Although the findings are interesting, this reviewer has major concerns about the experimental design, methodology, results, and interpretation of the data. Experimental details are lacking, including basic information (age, sex, strain of mice, procedures, magnification, etc.).*

We thank the reviewer for this important recommendation. We agree that comprehensive reporting of experimental details is essential for rigor and reproducibility.

In the revised manuscript, we added complete information regarding mouse strain, sex, age, and sample size for each experiment. In addition, detailed descriptions of surgical procedures, viral constructs, injection parameters, imaging magnification, and analysis methods have been incorporated into the Methods section.

These revisions ensured that all experiments are described with sufficient technical detail and clarity to allow accurate interpretation and replication of our findings. Experimental details have been incorporated, and corresponding revisions are highlighted for ease of review.

> ***Reviewer #3 (Recommendations for the authors):***
>
> *Addressing a few questions might help:*
>
> *(1) The study found that liver-associated LPGi neurons are predominantly GABAergic. It would be informative to molecularly characterize the PRV-traced, liver-projecting LPGi neurons to determine their neurochemical phenotypes.*

We thank the reviewer for this insightful suggestion. We agree that molecular characterization of liver-projecting LPGi neurons is important for understanding their functional identity.

This issue has been addressed in detail in our recent study (Cell Metab. 2025;37(11):2264-2279.e10), in which we performed single-cell RNA sequencing on retrogradely traced LPGi neurons connected to the liver. These analyses demonstrated that the majority of liver-projecting LPGi neurons are GABAergic, with a defined transcriptional profile distinct from neighboring non–liver-related populations.

Based on these findings, the current study selectively targeted GABAergic LPGi neurons using GAD1-Cre mice. We have explicitly cited these molecular results in the revised manuscript to clarify the neurochemical identity of the PRV-traced LPGi neurons. New text has been incorporated, and corresponding revisions are highlighted for ease of review.

> *(2) Is it possible to do a local microinjection of a sodium channel blocker (e.g., lidocaine) or an adrenergic receptor antagonist into the porta hepatis? That would potentially provide additional evidence for the porta hepatis as the functional crossover point.*

We appreciated the reviewer's thoughtful suggestion. Although pharmacological blockade at the porta hepatis can modulate local neural activity, this approach is inherently limited in its ability to distinguish between ipsilateral and contralateral inputs. Consequently, it may not provide definitive evidence for neural crossover at this specific site.

In our view, the anatomical evidence provided by whole-mount tissue clearing, dual-labeled tracing, and direct visualization of decussating nerve bundles at the porta hepatis offers a more definitive demonstration of sympathetic crossover. Pharmacological blockade would affect both crossed and uncrossed fibers simultaneously and therefore would not specifically resolve the anatomical organization of this decussation.

Nevertheless, we agree that functional interrogation of the porta hepatis represents an interesting direction for future work, and we acknowledge this possibility in the Discussion (Paragraph 6: "Fourth, although our data support a peripheral decussation at the porta hepatis, direct validation of this crossover site was not feasible with local pharmacological blockade, as currently available approaches lack sufficient spatial specificity and would likely perturb multiple neural components. Future studies employing more selective inhibitory strategies will be required to directly test this possibility.").

> *(3) It is possible to investigate the effects of unilateral LPGi manipulation or ablation of one side of CG/SMG on liver metabolism, such as hyperglycemia?*

We thank the reviewer for this important suggestion. Because unilateral LPGi manipulation was already examined in our study (Figure 2D), we focused here on unilateral ablation of the CG to further assess lateralized sympathetic control of hepatic metabolism. We successfully performed unilateral CG ablation without LPGi manipulation, but observed no significant change in blood glucose compared with the sham group (Author response image 3A and 3B). To determine whether glucose homeostasis was nonetheless affected, we further performed glucose tolerance tests (GTT) and insulin tolerance tests (ITT) (Author response image 3C and 3D). Neither test showed significant impairment after unilateral ablation, suggesting that compensatory neural mechanisms and/or hormonal homeostatic regulation may be recruited to preserve systemic glucose homeostasis.

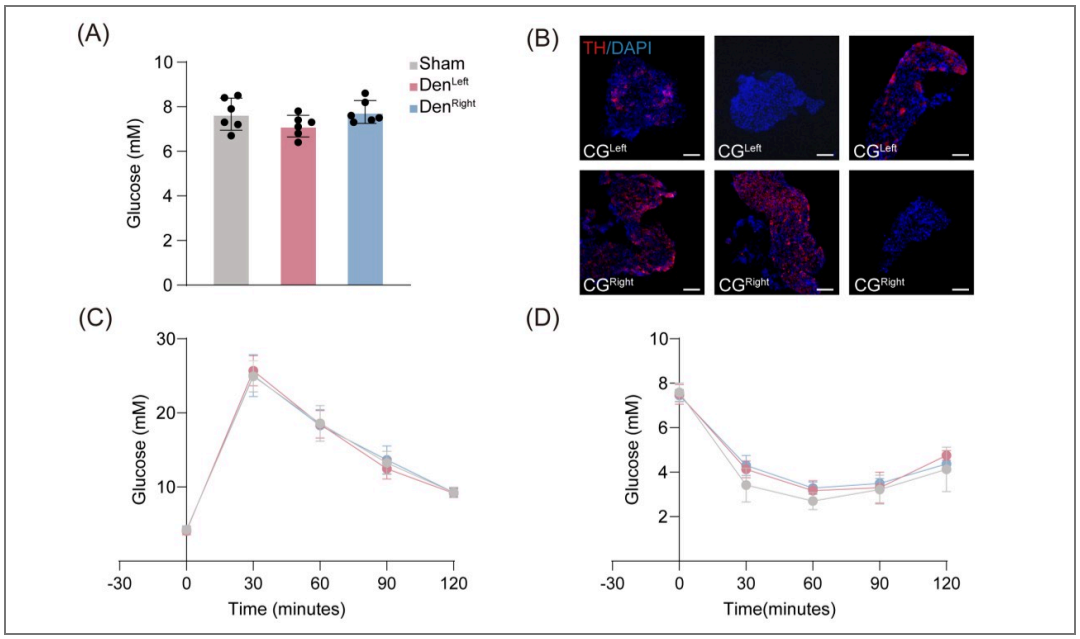

Author response image 3. (A) Blood glucose levels in mice subjected to left- or right-sided CG ablation via 6-OHDA treatment (n = 6). (B) Representative images of ablation of CG. Scale bars, 100 μm. (C and D) Blood glucose levels during GTT (C, n = 6) and ITT (D, n = 6) in mice with left- or right-sided CG ablation.

> ***Reviewer #4 (Recommendations for the authors):***
>
> *In the abstract and elsewhere, the use of the term 'sympathetic release' is unclear - do you mean release of nerve products, such as the neurotransmitter norepinephrine? This should be more clearly defined.*

We thank the reviewer for pointing out this ambiguity. We agree that the term “sympathetic release” was imprecise. In the revised manuscript, we explicitly referred to the release of sympathetic neurotransmitters, primarily norepinephrine, from postganglionic sympathetic fibers.

We revised the wording throughout the manuscript to ensure accurate and consistent terminology and to avoid potential confusion regarding the underlying neurobiological mechanisms.

Original: “Following unilateral hepatic denervation, contralateral LPGi activation induced metabolic compensation in the remaining innervated lobes, characterized by increased sympathetic release, glucose production, and glycogen depletion.”

Revised: “Following unilateral hepatic denervation, contralateral LPGi activation induced metabolic compensation in the remaining innervated lobes, characterized by increased norepinephrine release, glucose production, and glycogen depletion.”

https://doi.org/10.7554/eLife.109599.2.sa0